The role of Notch and Integrin-β1 signaling in muscle development

Inaugural-Dissertation

to obtain the academic degree

Doctor rerum naturalium (Dr. rer. nat.)

submitted to the Department of Biology, Chemistry and Pharmacy of Freie Universität Berlin

by

Maciej Czajkowski

from Poznań, Poland

June, 2014

This work was carried out at the Max-Delbrück-Center for Molecular Medicine from September 2008 to June 2014 under the supervision of Prof. Dr. Carmen Birchmeier.

1st Reviewer: Prof. Dr. Carmen Birchmeier
2nd Reviewer: Prof. Dr. Fritz Rathjen

Date of defense: 13.10.2014

Acknowledgments

I would like to thank Prof. Dr. Carmen Birchmeier for giving me the opportunity to work in her research group, for the constructive supervision and support. I thank Prof. Dr. Fritz Rathjen for being my thesis advisor.

I thank my colleagues in the laboratory for the collaboration and critical discussions. I am grateful to Dr. Elena Vasyutina for introducing me to the experimental techniques used for muscle analysis. I would like to thank Claudia Raßek and Dr. Ines Lahmann for fruitful collaboration in the analysis of genetic interactions of *Integrin-β1* and *Rac1*. I thank Dr. Dominique Bröhl for careful reading and editing the thesis. I thank Claudia Päseler, Petra Stallerow, Iris Falk and Katharina Werner for help with the animal husbandry.

Table of contents

1 Introduction

1.1 The function of craniofacial muscles

Approximately 60 distinct skeletal muscles exist in the vertebrate head, for instance the extraocular, facial, laryngeal, masticatory and tongue muscle. The seven extraocular muscles locate in each eye orbit and derive from cranial mesoderm. Two oblique muscles and four rectus muscles are responsible for the movement of the eye in horizontal, vertical and torsional axes. The seventh extraocular muscle, the *levator palpebrae superioris* muscle, elevates and retracts the upper eyelid. Mastication muscles are first arch-derived muscles that move the jaw and, in addition, participate in sound production. They include the temporalis muscle, medial and lateral pterygoid muscles, and the masseter muscle. The mimetic muscles are second arch-derived muscles that control facial expression. The tongue consists of eight muscles. Four intrinsic muscles, which are not attached to a bone, change the shape of the tongue during talking and swallowing. The extrinsic muscles attach to a bone and extend into the tongue, which they protrude, retract, depress, and elevate (Fig. 1).

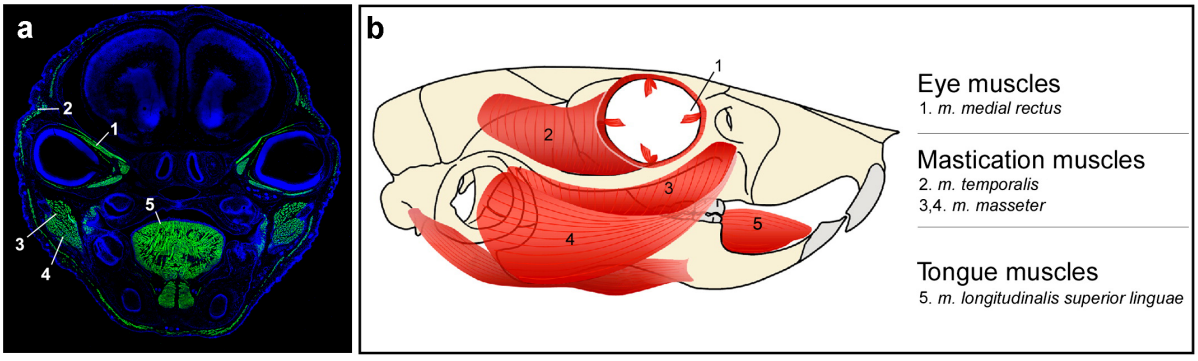

Figure 1. The anatomy of craniofacial muscles in mice.
(a) Section of an E18 embryonic head stained for the muscle marker myosin (green). Nuclei were counterstained with DAPI (blue). Distinct muscles are marked and shown schematically in (b). (b) Anatomical cartoon of the adult mouse head, highlighting the craniofacial muscles shown also in (a). Adapted from (Harel et al., 2009).

1.2 Development of the muscles in vertebrates

Skeletal muscles of the body and extremities derive from somites, which are ball-like structures that develop from the paraxial mesoderm on both sides of the neural tube. Somites differentiate under the influence of signals from the surrounding tissues, the skin and the notochord, and generate sclerotome and dermomyotome (Aoyama and Asamoto, 1988; Christ et al., 1992; McMahon et al., 1998; Reshef et al., 1998). The sclerotome gives rise to vertebrae and ribs, and the dermomyotome generates all skeletal muscles of the trunk and limbs as well as the dermis of the back skin (Christ and Ordahl, 1995). Myogenesis is initiated at the dorsomedial quadrant of the somites, followed by muscle cell differentiation at the medial and lateral dermomyotomal lips (Ben-Yair and Kalcheim, 2005; Gros et al., 2005). Cells originating from the medial lip give rise to the epaxial muscles, and cells from the lateral lip generate hypaxial muscles (Ordahl, 1992).

The origin of the head muscles is different than that of body and limb muscles, and they appeared later in evolution than trunk muscles. Most craniofacial muscles derive from the morphologically non-segmented mesoderm of the head (Noden, 1983; Couly et al., 1992; Harel et al., 2009).

The pharyngeal mesoderm is divided into two subdomains: (i) cranial paraxial mesoderm that is positioned along the neural tube and notochord and formed by loosely connected cells, and (ii) splanchnic lateral mesoderm that maintains an epithelial shape and that lies adjacent to the cranial paraxial mesoderm (Noden and Trainor, 2005; Tzahor and Evans, 2011). The border between the two subdomains is not clearly defined early in development (Fig. 2).

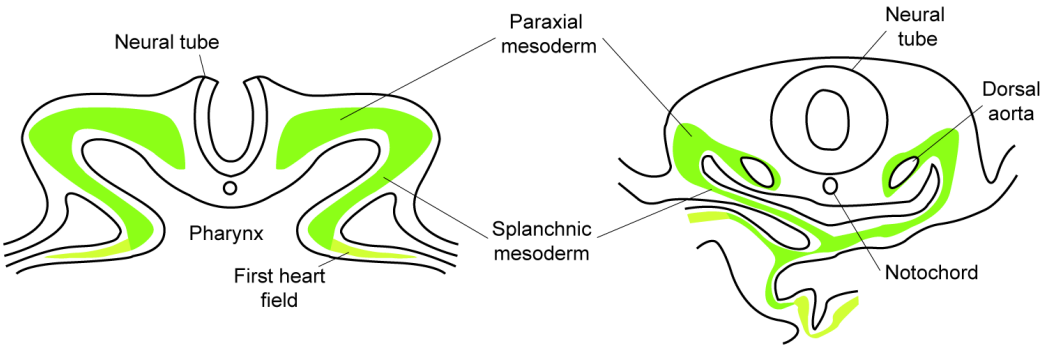

Figure 2. Pharyngeal mesoderm cells give rise to parts of the heart and the pharyngeal muscles.
Schematic illustration of the anatomy of the pharyngeal mesoderm in a 1.5–2-day-old chick embryo. Pharyngeal mesoderm cells (green) in the anterior part of the embryo surround the pharynx. Later, these cells fill the core of the pharyngeal arches, and are incorporated into arterial pole of the heart. Adapted from (Tzahor and Evans, 2011).

Later in development, the splanchnic lateral mesoderm locates to the ventral side of the embryo and beneath the floor of the pharynx. Cranial paraxial mesoderm cells display skeletal muscle potential, while lateral splanchnic lateral mesoderm cells contribute mostly to the heart. Cranial paraxial mesoderm and splanchnic lateral mesoderm merge into a mesodermal core within pharyngeal arches (also known as branchial arches), and eventually form first and second pharyngeal arch-derived muscles (branchiomeric muscle). Extraocular muscles are non-branchiomeric muscles and originate probably from the cranial paraxial mesoderm (Grifone and Kelly, 2007; Nathan et al., 2008; Tzahor, 2009). In contrast, tongue and neck muscles are of mixed origin. Intrinsic tongue muscles originate mainly from occipital somites, whereas extrinsic muscles and the proximal component of intrinsic tongue muscles derive mainly from the head mesenchyme (Huang et al., 1999; Harel et al., 2009).

1.3 Heterogeneity of muscle satellite cells

The adult muscle possesses an impressive regenerative potential (Buckingham, 2006). The cellular sources responsible for regeneration are satellite cells, the stem cells of the muscle. Satellite cells are defined by their localization, i.e. as

cells wedged between the myofiber and the basal membrane of muscle fibers (Mauro, 1961). Satellite cells proliferate in the perinatal phase, but reach quiescence in the adult. Upon injury, satellite cells are activated and begin to proliferate, generating daughter cells that undergo myogenic differentiation. In addition, satellite cells also self renew, generating cells that retain a stem cell character (Bischoff and Heintz, 1994; Conboy and Rando, 2002; Zammit et al., 2004; Collins et al., 2007).

Like the muscle they associate with, satellite cells derive from different mesodermal lineages: the somitic $Pax3^+$ lineage gives rise to satellite cells in the trunk and limbs, the $Mesp1^+$ cranial mesodermal lineage generates satellite cells in extraocular and branchiomeric muscles, and the $Isl1^+$ lineage from the splanchnic lateral mesoderm generates satellite cells of mastication muscles (Harel et al., 2009). Satellite cells in trunk and head muscle are also functionally different. For instance, satellite cells of the jaw muscle (*musculus masseter*) display delayed differentiation and increased proliferation compared to satellite cells from a leg muscle (*musculus extensor digitorum longus*) (Ono et al., 2010). When satellite cells from extraocular muscles are transplanted into the *tibialis anterior* muscle, they form fibers and also self-renew to generate new satellite cells. However, these new fibers produced by transplanted satellite cells no longer express markers specific to the extraocular lineage (Sambasivan et al., 2009).

1.4 Distinct genetic programs of craniofacial and trunk myogenesis

The myogenic regulatory factors MyoD, Myf5 and Mrf4 cooperate to control the entry into the myogenic differentiation program, and all muscle groups are absent in mutants that lack the expression of all three factors (Rudnicki et al., 1993; Kassar-Duchossoy et al., 2004). However, different transcriptional mechanisms control expression of the myogenic regulatory factors and therefore entry into the

differentiation program in trunk and craniofacial muscle (Rudnicki et al., 1993; Tajbakhsh et al., 1997; Kelly et al., 2004). In particular, Pax3/7 and transcription factors of the Six family act upstream of myogenic regulatory factors in the muscles of the body and limbs (Gros et al., 2005; Kassar-Duchossoy et al., 2005; Relaix et al., 2005; Relaix et al., 2013), whereas Pitx2 and Tbx1 take over this function in craniofacial muscle (Kitamura et al., 1999; Kelly et al., 2004; Dong et al., 2006; Sambasivan et al., 2009). Mutation of *MyoD* leads to upregulated expression of *Myf5* and results ultimately in normal muscle development, indicating that *MyoD* and *Myf5* can largely compensate for each other (Rudnicki et al., 1992). Mice lacking both, *Myf5* and *Pax3*, develop normal craniofacial muscles, but trunk muscles are affected. Thus, *Pax3* is necessary for the expression of *MyoD* in the trunk but not in the head (Tajbakhsh et al., 1997). In the absence of *Myf5* and *Mrf4*, MyoD rescues muscle development in trunk muscles, while in the head only extraocular muscles are affected (Sambasivan et al., 2009).

Capsulin and MyoR mark undifferentiated facial muscle precursors cells (von Scheven et al., 2006). In *capsulin*/*MyoR* double mutant mice, the first arch-derived muscle precursors fail to activate expression of the myogenic regulatory factor genes. The cells undergo apoptosis, resulting in a disturbed formation of mastication muscles (Lu et al., 2002). MyoR and capsulin bind to regulatory elements of *MyoD* and *Myf5* and drive the expression of the genes in branchial arches (Moncaut et al., 2012). In the absence of *MyoR*, expression of *Myf5* and *MyoD* in the branchial arches is reduced at early stages, while *Tbx1* expression is increased (Moncaut et al., 2012).

Genetic studies revealed that *MyoR* and *capsulin*, together with *Tbx1* and *Pitx2* are major players upstream of the myogenic determination genes in head muscle. In *Tbx1* mutant mice, the pharyngeal muscle development is severely perturbed, and *Myf5* and *MyoD* fail to be correctly expressed (Kelly et al., 2004). Similar to the *capsulin*/*MyoR* double mutation, *Pitx2* ablation results in decreased

expression of *Myf5* and *MyoD*. Extraocular muscles and muscles of mastication are affected and MyoR-positive cells in the first branchial arch are lost (Kitamura et al., 1999; Dong et al., 2006).

The proposed model of the transcriptional regulation during arch myogenesis places *MyoR* and *capsulin,* together with *Tbx1* and *Pitx2*, upstream of *Myf5* and *MyoD* (Moncaut et al., 2012).

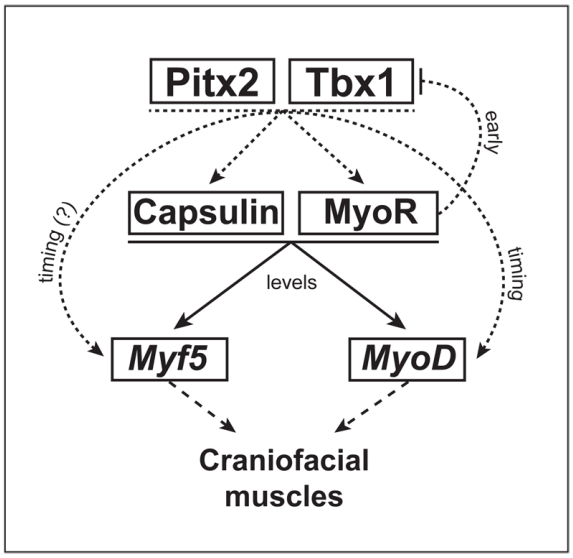

Figure 3. Proposed model for the transcriptional regulation of *Myf5* and *MyoD* during branchial arch myogenesis.
In branchial arches, Pitx2 and Tbx1 act as upstream factors in the myogenic cascade regulating the expression of *MyoR* and c*apsulin* in a direct or indirect fashion. The expression levels of the myogenic regulatory factors during early branchial arch development are controlled by the direct interaction of MyoR and capsulin with the regulatory regions of *Myf5* and *MyoD*. Although Pitx2 and Tbx1 could control the timing of activation of expression of *Myf5* and *MyoD*, the control of their expression levels probably takes place through the activation of MyoR and capsulin. Dashed arrows represent direct or indirect interactions; solid arrows represent direct interactions. Adapted from (Moncaut et al., 2012).

1.5 Notch signaling in muscle development

The Notch signaling cascade in vertebrates and invertebrates is evolutionarily highly conserved (Kimble and Simpson, 1997; Lewis, 1998; Artavanis-Tsakonas et al., 1999). The pathway is activated after binding of a ligand (Dll1, Dll3, Jag1,

Jag2 in mice) to the receptor (Notch1-4 in mice), which results in receptor cleavage, release of the Notch intracellular domain (NICD) and its translocation to the nucleus. Nuclear NICD directly interacts with the transcription factor Rbpj, and the interaction is required to activate target genes like *Hes1* and *Hey1*. Notch signaling has long been known to suppress myogenic differentiation in cultured C2C12 cells, primary satellite cells, and developing chick embryos (Kopan et al., 1994; Shawber et al., 1996; Kuroda et al., 1999; Delfini et al., 2000; Hirsinger et al., 2001; Conboy and Rando, 2002). In particular, Notch signaling is known to repress *MyoD* and induces *MyoR* in C2C12 cells (Kuroda et al., 1999; Buas et al., 2009).

Delta-like 1 (*Dll1*) is a member of the Delta/Serrate/lag-2 (DSL) family and is essential for cell-cell communication. *Dll1* is transiently expressed during embryogenesis in the nervous system and in the paraxial mesoderm (Bettenhausen et al., 1995). *Dll1* transcripts are detected in the skeletal muscles during development (Beckers et al., 1999). In limb buds, *Dll1* is expressed in myoblasts and myocytes but not in progenitor cells (Schuster-Gossler et al., 2007). A null mutation of *Dll1* ($Dll1^{LacZ}$) results in a disturbed somitogenesis and a disrupted arrangement of myotome and sclerotome, and the mutant mice die at E11 probably due to heart deficits (Hrabe de Angelis et al., 1997). Despite a strongly reduced Notch signaling activity, mice heteroallelic for the null ($Dll1^{LacZ}$) and a hypomorphic allele ($Dll1^{Ki}$) survive until birth. This leads to premature muscle differentiation and decrease of muscle growth, resulting in formation of tiny muscle groups in the trunk and extremities. The myogenic regulatory factors MyoD, MyoG and Mfr4 are transiently upregulated in the myotome and head muscles of the mutant embryos, indicating that differentiation of muscle cells in head muscles groups is increased as well (Schuster-Gossler et al., 2007). Similarly, mutation of *Rbpj* results in the depletion of the progenitor pool in fetal myogenesis due to their premature differentiation (Vasyutina et al., 2007).

Recently, work in the laboratory of Carmen Birchmeier showed that elimination of Notch signals during mouse development leads to the incorrect homing of the satellite cells in the trunk and limbs. The disrupted homing was a result of a deficit in basal lamina assembly around emerging satellite cells. In order to observe these late functions of Notch, the progenitor pool that is depleted early during development when *Dll1* or *Rbpj* are mutated had to be rescued. This was achieved by a mutation of the myogenic regulatory factor *MyoD*. In *Dll1*$^{LacZ/Ki}$*;MyoD* double mutant mice, the number of Pax3^{+} myogenic progenitor cells reached the levels observed in control mice, but the colonization of the satellite cell niche was severely disrupted (Bröhl et al., 2012).

1.6 Myoblast fusion in mice

Skeletal muscle fibers arise by the fusion of myogenic cells. The process of myogenesis occurs in two phases. Primary myogenesis occurs at embryonic day (E) 11 and forms initial fibers that contain few nuclei. Subsequently, secondary myogenesis generates additional fibers that locate around the primary fibers (Ontell and Kozeka, 1984; Duxson et al., 1989). During early secondary myogenesis, myoblasts fuse preferentially with primary myotubes, and at the end preferentially with secondary myotubes (Zhang and McLennan, 1995). Many molecules have been reported to be responsible for fusion *in vitro* by the use of blocking antibodies and siRNA studies, but only few of these could be confirmed *in vivo* (Horsley and Pavlath, 2004). *Integrin-β1* is a gene essential for fusion in mice, and was proposed to act as a component of the VLA-4/VCAM-1 complex in the regulation of fusion of myoblasts with myotubes during the late phases of secondary myogenesis (Rosen et al., 1992; Schwander et al., 2003).

Muscle growth occurs also in the adult and is mediated by satellite cells that share a developmental origin with embryonic muscle progenitors (Gros et al., 2005; Kassar-Duchossoy et al., 2005; Relaix et al., 2005). In a quiescent state, satellite cells are associated with the basal lamina of the muscle fiber. Upon

injury, the cells become activated, differentiate and fuse with other myoblasts or with damaged myofibers (Collins et al., 2005).

On a cellular level, fusion is characterized by adhesion, alignment of myoblast membranes, followed by the formation of a specialized membrane microdomain at the contact sites. Genetic analyses performed in *Drosophila* revealed a molecular cascade that controls actin polymerization to be essential for myoblast fusion. This cascade comprises Rac GTPases, Rac regulators, WASp nucleation promoting factor, and the Arp2/3 complex (Luo et al., 1994; Richardson et al., 2007; Schafer et al., 2007). The function of Rac1, N-Wasp and the Rac1 regulator Dock180 in myoblast fusion is conserved in mice, indicating that similar mechanisms control fusion in the entire animal kingdom. In *Drosophila*, adhesion of myoblasts is mediated by Ig-superfamily proteins (Bour et al., 2000; Ruiz-Gomez et al., 2000; Strunkelnberg et al., 2001). Whether adhesion molecules of the Ig-family play a role in myoblast fusion in mice is still open, and *in vitro* analyses showed that also other families of adhesion molecules might mediate myoblast fusion. Molecules with non-conserved functions are Integrin-β1 and the small GTP binding protein Cdc42, which are essential for myoblast fusion in mice but not in *Drosophila* (Schwander et al., 2003; Sohn et al., 2009; Vasyutina et al., 2009).

1.7 Structure and function of integrins

Integrins are heterodimeric transmembrane proteins that mediate cell-cell and cell-matrix adhesion. The integrin family consists of 18 alpha and 8 beta subunits forming 24 different non-covalently bound dimers. Each dimer consists of an extracellular domain that binds the ligand, a single membrane-spanning transmembrane domain, and an intracellular cytoplasmic tail domain linked to the actin cytoskeleton (Hynes, 2002). The diversity of the family is further increased by alternative mRNA splicing of sequences encoding both, intra- and extracellular domains (Ziober et al., 1993).

In the inactive state, the ligand-binding pocket of integrins is oriented towards the plasma membrane, which prevents ligand interaction. Activating signals inside the cell are provided by molecules like talin or kindlin (inside-out signaling). This induces opening of the structure and exposes the external ligand binding site to the ligands, allowing ligand binding and outside-in signaling (Luo and Springer, 2006). Ligand-bound integrins activate various cytoplasmic signaling molecules, among tyrosine kinases like Fyn and Src (outside-in signaling). These signals are potent regulators of cell growth and survival.

Extracellular matrix proteins are the major integrin ligands, for instance laminin, collagen, fibronectin and vitronectin. Focal adhesion sites assemble integrins that connect to the extracellular matrix and the actin cytoskeleton, and these structures have functions in cell motility and polarity (Geiger et al., 2001; Brakebusch et al., 2002). However, integrins are unable to bind actin without adaptor molecules, which interact with the cytoplasmic tail of integrins and mediate assembly of actin scaffolds. More than 42 cytoplasmic proteins were implicated in Integrin-β1-binding (Legate and Fassler, 2009).

1.8 Function of integrins in muscle differentiation

All beta and most of the alpha integrin subunits have been mutated in mice resulting in distinct phenotypes, ranging from defects in the kidney, lung, retina and blood vessels (Bouvard et al., 2001). The role of various integrin subunits in muscle differentiation has been previously investigated. Integrin-α4 was expected to participate in the formation of myotubes, acting together with Integrin-β1 in the recognition of the counter receptor VCAM-1 (Rosen et al., 1992). However, the early lethality of the *Integrin-α4*-deficient mice precluded an analysis in myoblast fusion (Yang et al., 1996), and unpublished data from the laboratory of Carmen Birchmeier indicates that VCAM-1 is dispensable for myoblast fusion.

Integrin-α7β1 is a laminin receptor mostly expressed in skeletal and cardiac muscles, which expression is strongly upregulated after myotube formation (Song et al., 1993). Mice lacking *Integrin-α7* showed typical symptoms of a progressive muscular dystrophy, with variation in fiber size, centrally located nuclei and hypertrophic fibers. Moreover, *Integrin-α7β1*-deficient mice revealed a severe disruption of myotendinous junctions (Mayer et al., 1997).

Although the expression of *Integrin-α5β1* and *Integrin-α6β1* is downregulated upon myoblast fusion, their role in myotube formation is different (Bronner-Fraser et al., 1992; Boettiger et al., 1995). Primary myoblasts in which the α5 subunit was overexpressed showed decreased differentiation and myoblasts were maintained in proliferative phase, while α6 overexpression inhibited proliferation but not myoblast differentiation (Sastry et al., 1996). *Integrin-α5*-deficient chimeric mice revealed alterations in skeletal muscles resembling a typical muscle dystrophy suggesting that α5β1 regulates muscle fiber integrity. However, $\alpha5^{-/-}$ myoblasts differentiate efficiently into myotubes (Taverna et al., 1998) and mice with a deletion of the α6 subunit show no obvious defects in muscle development (Georges-Labouesse et al., 1996). Other alpha chains (α1, α3 and αv) were reported not to have an impact on mouse myogenesis (Gardner et al., 1996; Kreidberg et al., 1996; Bader et al., 1998).

Due to contradictory studies it was unclear whether Integrin-β1 regulates myoblast fusion. β1-deficient mice die shortly after embryo implantation (Fassler and Meyer, 1995). Analysis of *Integrin-β1* chimeric mice demonstrated that muscle was formed normally. Myoblasts and satellite cells isolated from β1-null chimeric mice were able to fuse into multinucleated myotubes, although the fusion was delayed (Hirsch et al., 1998). On the other hand, an antibody against Integrin-β1 blocks sarcomere formation in developing myotubes (McDonald et al., 1995). To address the function of Integrin-β1 in myogenesis, conditional mutant mice were generated (Graus-Porta et al., 2001). The gene was deleted in

skeletal muscles using Cre recombinase under control of the human skeletal alpha-actin (HSA) promoter (Brennan and Hardeman, 1993). In such mice, the *Integrin-β1* recombination is beginning in the myotome around embryonic day 9.5. Pronounced deficits of diaphragm and intercostal muscles were detected, as well as accumulation of unfused cells in the limb muscles at E16.5. Although migration, proliferation and differentiation of the myoblasts were not impaired, conditional *Integrin-β1* mutant muscle contained fewer fibers, and isolated mutant cells in culture did not efficiently fuse into myotubes. Electron microscopy revealed that *Integrin-β1*-deficient myoblasts adhere to each other, but membrane breakdown associated with fusion was rarely observed. Moreover, tetraspanin CD9 protein was not expressed at the cell surface of the mutant myoblasts. These data suggest that Integrin-β1 is not required for cell-cell interaction between myoblasts, but is essential for myoblast fusion (Schwander et al., 2003).

1.9 Integrin-linked kinase in skeletal muscle development

Integrin-linked kinase (ILK) is located in focal adhesions and plays a crucial role in maintaining connections between the actin cytoskeleton and the plasma membrane (Yamaji et al., 2001). ILK is multidomain adaptor protein composed of ankyrin (ANK) repeats, a pleckstrin homology (PH) domain and Ser/Thr kinase domain. The first ANK domain binds the LIM-domain-only proteins like PINCH1 and PINCH2 (Zhang et al., 2002; Braun et al., 2003), which interacts with SH2/SH3-containing adaptor protein Nck2 (Tu et al., 1998). The Ser/Thr kinase domain interacts with Integrin-β1, paxillin and parvin (Nikolopoulos and Turner, 2000; Olski et al., 2001; Tu et al., 2001). ILK and the adaptor proteins PINCH and parvin form heterotrimeric complex recruiting actin along with components of several signaling pathways to sites of focal adhesions in fibroblasts (Hannigan et al., 2005; Wu, 2005; Legate et al., 2006). *ILK*-deficient cells show a severe delay in formation of focal adhesion, which results in defective cell spreading (Sakai et

al., 2003). In addition, ILK was shown to regulate integrin-associated rearrangement of actin filament through a phosphatidylinositol 3-kinase/Akt/Rac1 pathway (Qian et al., 2005).

ILK-null mice die shortly after implantation due to impaired epiblast polarization and abnormal F-actin accumulation (Sakai et al., 2003). Conditional ILK-deficient mice crossed with a mouse strain expressing Cre recombinase under the control of the HSA promoter developed a mild progressive muscular dystrophy, but myotube formation was not impaired. The phenotype was detected mostly in myotendinous junctions with detachment of the basement membrane from the sarcolemma, variation of muscle fiber size and increased fibrosis, suggesting that ILK plays a critical role in stabilizing integrin-actin interaction. With the caveat that the mutation was introduced relatively late during the differentiation with the HSA^{Cre} line employed in this study, the data indicate that ILK does not play a role in myoblast fusion but is essential for myotendinous junction formation (Wang et al., 2008).

1.10 Aim of the study

The role of Notch signaling in the development of the trunk muscle has been previously investigated in mice. In this study, I analyzed the function of Notch signaling in craniofacial myogenesis. I determined the expression pattern of *Dll1* ligand in the mouse head. I used the $Dll1^{LacZ/Ki}$ mutant strain to investigate the role of Notch signaling in the maintenance and homing of muscle progenitor cells. In particular, I investigated whether the mutation of the myogenic regulatory factor MyoD results in the rescue of the *Dll1* phenotype. In addition, I defined the Notch-dependent expression of *MyoR* involved in specification of craniofacial muscle progenitor cells.

Fusion of myoblasts into multinucleated myotubes plays an essential role in muscle function. It contributes to muscle growth and regeneration of myofibers upon injury. To better understand the process, I compared conditional *Integrin-β1*

and *ILK* mutant mice. I characterized the migration of myogenic progenitor cells into the extremities and quantified fusion deficits in conditional mutant mice when *Integrin-β1* and *ILK* were ablated early during myogenesis using $Pax3^{Cre}$ for conditional mutagenesis.

2 Materials and methods

2.1 Abbreviations

°C	degree Celsius
AP	alkaline phosphatase
BCIP	5-Bromo-4-chloro-3-indolyl-phosphate
BSA	Bovine serum albumin
cDNA	complementary DNA
DAPI	4',6-diamidino-2-phenylindole
ddH_20	double distilled water
DIG	Digoxigenin
Dll1	Delta like 1
DMEM	Dulbecco's Modified Eagle Medium
DMSO	Dimethylsulfoxide
DNA	Deoxyribonucleic acid
dNTPs	Deoxyribonucleotide triphosphate
DTT	dithiothreitol
E	embryonic day
EDTA	Ethylene diamine tetraacetic acid
et al.	*et altera*
FACS	Fluorescence-activated cell sorting
fw	forward
g	gram
h	hour
H_20_2	Hydrogen peroxide
HBSS	Hank's Balanced Salt Solution
HCl	Hydrochloric acid
HEPES	4-(2-hydroxyethyl)-1-piperazineethanesulfonic acid
HS	horse serum
Igepal	octylphenoxypolyethoxyethanol

l	liter
LacZ	b-galactosidase coding sequence
LB	Luria-Bertani medium
M	Molar
MgCl2	Magnesium chloride
min	minute
ml	milliliter
NaCl	Sodium chloride
NaOH	Sodium hydroxide
NBT	Nitro blue tetrazolium chloride
NTMT	Alkaline phosphatase buffer
PBS	Phosphate buffered saline
PCR	Polymerase chain reaction
PFA	Paraformaldehyde
pH	*potentium hydrogenii*
PVA	Polyvinyl alcohol
qPCR	quantitative polymerase chain reaction
rev	reverse
RIPA	Radioimmunoprecipitation assay buffer
RNA	Ribonucleic acid
RNase	Ribonuclease
SDS	Sodium dodecyl sulfate
SSC	Saline sodium citrate
Tris	2-Amino-2-(hydroxymethyl)-propane-1,3-diol
Triton X100	polyethylene glycol p-(1,1,3,3-tetramethylbutyl)-phenyl ether
tRNA	transfer ribonucleic acid
TSA	Tyramide signal amplification
Tween-20	Polyoxyethylene (20) sorbitan monolaurate
U	Unit
UV	Ultraviolet
µm	microliter

2.2 Materials

2.2.1 Chemicals

All chemicals, materials, oligonucleotides and kits for molecular biology were purchased from following companies: Ambion (Austin, USA), Biochrom (Berlin), BD Biosciences (Franklin Lakes, USA), DakoCytomation (Glostrup, DK), Dianova (Hamburg), Gibco (Darmstadt), Invitrogen (Karlsruhe), Marienfeld (Lauda-Königshofen), Molecular Research Center (Cincinnati, USA), MWG Eurofins (Ebersberg), New England Biolabs (Ispwich, USA), PAN-Biotech (Aidenbach), Partec (Münster), PerkinElmer Life Sciences (Boston, USA), Promega (Madison, USA), Roche (Basel, CH), Roth (Karlsruhe), R&D Systems (Minneapolis, USA), Sakura Finetek (Torrance, USA), Santa Cruz Biotechnology (Santa Cruz, USA), Serva (Heidelberg), Sigma-Aldrich (St. Louis, USA), Thermo Scientific (Waltham, USA), Qiagen (Hilden), Vector Laboratories (Burlingame, USA).

2.2.2 Bacterial strains

Escherichia coli DH10B	F- endA1 recA1 galE15 galK16 nupG rpsL ΔlacX74 Φ80lacZΔM15 araD139 Δ(ara,leu)7697 mcrAΔ (mrr-hsdRMS-mcrBC) λ-

2.2.3 Vectors

Name	**Source**
pGEM-T Easy	Promega

2.2.4 DNA-oligonucleotides

Oligonucleotides were synthesized by MWG Eurofins, Ebersberg.

2.2.4.1 Oligonucleotides used for genotyping

Name	Sequence 5'-3'
LacZ-fw	TCCCAACAGTTGCGCAGCCTGAATG
LacZ-rev	ATATCCTGATCTTCCAGATAACTGCCG
Dll1ki-fw	TGGATGTGGAATGTGTGCGAG
Dll1ki-rev	AAGGGGAGAAGATGCTTGATAACC
MyoD-WT-fw	ATGCAAGGACAGCGCTGGGGTTCTAA
MyoD-WT-rev	CCGTCGGGGCCTGTCAAGTCTATG
MyoD-Mut-fw	ACCCCAAGCTCCGCCCTACACTC
MyoD-Mut-rev	GCAGCGCATCGCCTTCTATC
Itgb1-fw	ACCCCTGCAGGCTCCTTGGAA
Itgb1-rev	CAGGACAAGCCGCCACAGCTT
ILK-fw	GTCTTGCAAACCCGTCTCTGCG
ILK-rev	CAGAGGTGTCAGTGCTGGGATG
Pax3Cre-fw	AGCACCTTTGCCAGTAGCC
Pax3Cre-rev	AATCGCGAACATCTTCAGGT
RosaYFP-1	AAAGTCGCTCTGAGTTGTTAT
RosaYFP-2	GCGAAGAGTTTGTCCTCAACC
RosaYFP-3	GGAGCGGGAGAAATGGATATG

2.2.4.2 Oligonucleotides for cloning of cDNAs for *in situ* riboprobes

Name	Sequence 5'-3'
MyoR-fw	GTGAGTGACCCCGAAGACTC
MyoR-rev	CTGTTGGCTGCAGAAACGTC
Dll1-fw	CTTCCCTCTGTGTCTTATC
Dll1-rev	GCAGGGCAGAGACCACGGC
Pitx2-fw	ATGTACCCCGGCTATTCGT
Pitx2-rev	TTCTAGCACAATTCTCAG
Tbx1-fw	AAGAAGAACCCGAAGGTGGC
Tbx1-rev	CGTGATCCGGTGATTCTGGT

2.2.4.3 Oligonucleotides used for quantitative PCR

Name	Sequence 5'-3'
Hes1-fw	CAGACATTCTGGAAATGACTGTGAA
Hes1-rev	CGCGGTATTTCCCCAACAC
Dll1-fw	GATACACACAGCAAACGTGACACC
Dll1-rev	TTCCATCTTACACCTCAGTCGCTA
Notch1-fw	CAAGAGGCTTGAGATGCTCC
Notch1-rev	AAGGATTGGAGTCCTGGCAT
Rbpj-fw	CTCAGCAAGCGGATAAAGGTCA
Rbpj-rev	GATGTAAAATGCTCCCCACTGTTG
Hey1-fw	GCCGACGAGACCGAATCAATAACA
Hey1-rev	TCCCGAAACCCCAAACTCCGATAG
Notch3-fw	ACTGCAGTGCTGGCGTCTCTTCAA
Notch3-rev	CATCCCAGCCGCATTCCTCAGTGTT
Pax7-fw	AGCAATGGCCTGTCTCCTC
Pax7-rev	ACGTGGGCAAGCTGTCTCCTG
β-actin-fw	GTCCACACCCGCCACCAGTTC
β-actin-rev	GGCCTCGTCACCCACATAG

2.2.5 Antibodies

Antigen	Host animal	Dilution	Source
Skeletal-fast myosin	mouse	1:200	Sigma-Aldrich
Laminin	rabbit	1:1000	Sigma-Aldrich
Desmin	goat	1:500	Santa Cruz
MyoD	rabbit	1:1000	Santa Cruz
MyoG	mouse	1:200	DakoCytomotion
Pax7	guinea-pig	1:2500	J. Griger (MDC, Berlin)
GFP	rat	1:1500	Nacalai Tesque
Lbx1	guinea pig	1:20000	T. Müller (MDC, Berlin)
Caspase-3, cleaved	rabbit	1:300	Cell Signaling

Secondary antibodies conjugated with Cy2, Cy3, Cy5 (Dianova, 0.5mg/ml) or Alexa Fluor 488 and 555 (1:500) (Invitrogen).

2.2.6 Mouse strains

Dll1^{LacZ}

(Achim Gossler, The Jackson Laboratory, Bar Harbor, USA) homologous recombination of amino acids 2-116 with in-frame fusion of *LacZ* gene of *E. coli* (Hrabe de Angelis et al., 1997)

Dll1^{Ki}

(Achim Gossler, The Jackson Laboratory, Bar Harbor, USA) hypomorphic allele of *Dll1* gene (Schuster-Gossler et al., 2007)

MyoD$^{-/-}$

(Rudolf Jaenisch, Whitehead Institute and Department of Biology Massachusetts Institute of Technology, Cambridge, USA) deletion of exon 1 and half of intron 1 prevents the formation on an active polypeptide (Rudnicki et al., 1992)

Integrin-β1$^{flox/flox}$

(Reinhard Fässler, Max Plank Institute of Biochemistry, Martinsried) deletion of exon 2 to exon 7 upon Cre-mediated recombination (Potocnik et al., 2000)

ILK$^{flox/flox}$

(Reinhard Fässler, Max Plank Institute of Biochemistry, Martinsried) deletion of exon 2 containing ATG start codon upon Cre-mediated recombination (Grashoff et al., 2003)

Pax3^{Cre}

(Jonathan A. Epstein, University of Pennsylvania, Philadephia, USA) Cre recombinase gene sequence was inserted into the exon 1 of *Pax3* gene (Engleka et al., 2005)

Rosa^{YFP}

(Frank Costantini, Columbia University Medical Center, New York, USA) *Rosa^{YFP}* targeting vector contained *loxP*-flanked neomycin resistance gene upstream of enhanced *YFP* cDNA. The *Neo-YFP* sequence was flanked by the *Rosa26* genomic sequences (Srinivas et al., 2001)

2.2.7 Buffers and solutions

2.2.7.1 Bacterial culture:

LB-medium:

10g NaCl
10g Bacto-Tryptone
5g bacterial extract
ddH_2O to 1000ml
pH 7.5
Ampicillin – final concentration 100µg/ml

2.2.7.2 Buffers used for nucleic acid preparation:

Buffer I (Birnboim and Doly, 1979)

3.03g Tris base
1.86g EDTA*2H_2O
ddH_2O to 400ml
RNase 100µg/ml

Buffer II

4g NaOH
1% SDS
ddH_2O to 500ml

Buffer III

147.25g potassium acetate
ddH_2O to 500ml

pH adjusted to 5.5 with acetic acid

Proteinase K (10mg/ml)

10mg proteinase K per 1ml of ddH_2O

0.5M EDTA pH 8.0

146.1g EDTA

ddH_20 to 1000ml

pH adjusted to 8.0 with NaOH

1M Tris pH 7.5/ pH 8.0/ pH 9.5

211.9g Tris

ddH_20 to 1000ml

pH adjusted with HCl

5M NaCl:

292.2g NaCl in 1000ml ddH_20

4M NaOH:

160g NaOH in 1000ml ddH_20

1M $MgCl_2$:

203.3g $MgCl_2$ in 1000ml ddH_20

10% SDS:

10g SDS in 100ml ddH_20

10x TE-buffer:

50ml 1M Tris pH 7.5

10ml 0.5M EDTA pH 8.0

ddH_20 to 500ml

3M Sodium acetate pH 5.3:

24.6g sodium acetate in 100ml ddH_20

pH adjusted to 5.3 with acetic acid

DNA-lysis buffer:

2.5ml 1M Tris pH 7.5

5ml 0.5M EDTA pH 8.0

0.5ml 5M NaCl

15.5ml 10% SDS

ddH_20 to 250ml

2.2.7.3 Buffers for *in situ* hybridization:

10% Tween 20:

10ml Tween 20 to in 100ml ddH_20

PBT:

100ml 10x PBS

10ml 10% Tween 20

20x SSC pH 4.5/ pH 7.0:

175.3g NaCl

88.2g sodium citrate

ddH_20 to 1000ml

pH adjusted with HCl

NTMT:

60ml 1M Tris pH 9.5

12ml 5M NaCl

30ml 1M $MgCl_2$

600µl Tween 20

ddH_20 to 600ml

MAB 5x pH 7.5:

50g maleic acid

43.5g NaCl

ddH_20 to 1000 ml

adjust pH to 7.5 with NaOH

MABT:

100ml 1M maleic acid

30ml 5M NaCl

5ml 10% Tween 20

ddH_20 to 1000ml

Denhardt's solution 100x:

2g Ficoll 400

2g polyvinylpyrolidone

2g BSA (Roth)

filtered and stored at -20°C

Acetylation buffer:

2ml triethanolamine

0.25ml 37% HCl

0.375ml acetic anhydride

ddH_20 to 150ml

B1 buffer:

0.1M Tris pH 7.5

0.15M NaCl

Blocking solution:

10% goat serum in B1 buffer

***In situ* staining solution:**

50% of 10% PVA

50% 2x NTMT

1µl NBT/1ml

1µl BCIP/1ml

Hybridization buffer:

50% deionized formamide

5x SSC

5x Denhardt's solution

150µg/ml yeast tRNA

150µg/ml salmon sperm DNA

Hybridization buffer for whole mount *in situ* hybridization:

20ml formamide

12.5ml 20x SSC pH 4.5

25ml 100mg/ml heparin

500µl 10% Tween 20

ddH_20 to 50ml

Proteinase K buffer:

1ml 1M Tris pH 7.0

0.1ml 0.5M EDTA pH 8.0

10µg/ml proteinase K

PBT to 50ml

RIPA-buffer:

6ml 5M NaCl

2ml 1% Igepal

2ml 10% SDS

0.4ml 0.5M EDTA

10ml 1M Tris pH8.0

0.5% deoxycholate

ddH_20 to 200ml

SSC/FA/T buffer:

60ml 20x SSC pH 4.5

6ml 10% Tween 20

300ml formamide

ddH_20 to 600ml

Alkaline phosphatase buffer:

4ml 5M NaCl

10ml 1M $MgCl_2$

2ml 10% Tween 20

20ml 1M Tris pH 9.5

0.1g tetramisole hydrochloride

ddH_20 to 200ml

Fixing solution:

50ml 4% PFA

400µl 20% glutaraldehyde

0.5ml 10% Tween 20

0.5ml 0.5M EDTA pH 8.0

2.2.7.4 Buffers for immunohistochemistry:

10% BSA:

10ml BSA (Roth) in 100ml ddH_20

10% Triton X-100:

10ml Triton X-100 (Sigma-Aldrich) in 100ml ddH_20

1M Na_2HPO_4

177.95g in 1000ml ddH_20

1M NaH_2PO_4

156.01g in 1000ml ddH_20

4%/ 16% Paraformaldehyde (PFA):

20g/ 80g paraformaldehyde (Roth)

5ml 10x PBS (Gibco BRL)

ddH_20 to 500ml

adjust pH to 7.4 with NaOH

0.2M Na-phosphate buffer (2x):

154.8ml 1M Na_2HPO_4

45.2ml 1M NaH_2PO_4

ddH_20 to 1000ml

adjust pH to 7.3 with NaOH

Zamboni's fixative:

150ml 16% PFA

150ml picric acid (saturated solution)

500ml 0.2M Na-phosphate buffer

ddH_20 to 1000ml

TSA blocking solution:

10ml 10x PBS

10ml 100% HS (Biochrom)

0.1ml 100% Triton X-100

0.5g TSA blocking reagent (PerkinElmer Life Sciences)

ddH_20 to 100ml

Staining buffer:

300µl 100% HS

300µl 10% BSA

50µl 20% Triton X-100

1x PBS to 10ml

DAPI (1000x):

1mg/ml in 1x PBS

2.2.7.5 Buffers for satellite cell isolation:

Digestion medium:

DMEM 1g/l glucose, +pyruvate, +GlutaMAX (Gibco BRL) 500ml

12.5ml 1M HEPES pH 7.0 (PAN-Biotech)

2.5ml 10mg/ml gentamicin (Gibco BRL)

Staining buffer:

2.5ml 1M HEPES

5ml 10% BSA

0.4ml 0.5M EDTA pH 8,0

0.5ml 10mg/ml gentamicin (Gibco BRL)

91.6ml 1x HBSS (-$CaCl_2$, -$MgCl_2$) (Gibco BRL)

NB4 collagenase:

60mg NB 4G proved grade from *Clostridium histolyticum* collagenase (Serva)

HBSS to 10ml (Gibco BRL)

aliquot and freeze in -20°C

Dispase II (100U/ml):

0.1g Dispase II (Roche)

10ml HEPES-buffered saline (50mM HEPES-KOH pH 7.4, 150mM NaCl)

aliquot and freeze in -20°C

Trypsin:

8ml 2.5% trypsin (Gibco)

HBSS (-$CaCl_2$, -$MgCl_2$) to 100ml

2.2.7.6 Cell culture medium:

DMEM 4.5g/l glucose, +pyruvate, +GlutaMAX (Gibco BRL) 500ml

5%-10% FCS (Sigma)

1% gentamicin (Gibco BRL)

2.3 Methods:

2.3.1 Extraction and purification of nucleic acids

2.3.1.1 Isolation of plasmid DNA

Small-scale plasmid preparation was performed using 2ml LB culture of transfected *E. coli*. Isolation was performed according to alkaline lysis method (Birnboim and Doly, 1979). Large-scale plasmid preparation was performed using 250ml LB culture and Plasmid Maxi kit (Qiagen). The concentration and the purity of DNA were determined by UV-spectrophotometer (Thermo Scientific).

2.3.1.2 Isolation of genomic DNA from mouse tissue

Ear and tail biopsies were lysed at 55°C in DNA-lysis buffer containing 1mg/ml proteinase K for 3h. The enzyme was inactivated by incubation at 95°C for 10 min. The samples were diluted with 250µl H_20. 1µl of genomic DNA was used for genotyping.

2.3.1.3 Isolation of RNA

FACS-isolated satellite cells were collected into 1600µl TRIzol reagent (Ambion). 2µl Polyacryl carrier (Molecular Research Center) was added to the samples and incubated 5 min at room temperature. After adding 300µl chloroform the samples were centrifuged for 15 min at 10^4xg at 4°C (Eppendorf 5417R centrifuge). The upper phase was collected and 600µl of isopropanol was added. The samples were incubated for 10 min at room temperature and centrifuged for 10 min at 12x10^3xg at 4°C. RNA pellet was washed with 75% ethanol and centrifuged for 5

min at 12x10^3xg at 4°C. The pellet was air-dried for 15 min and dissolved in 30µl of RNAse-free H_20.

2.3.1.4 cDNA synthesis

First strand DNA was synthesized using random hexamer primers, dNTPs, 5x First strand buffer, DTT, RNAse Out and Superscript III synthesis kit (Invitrogen).

2.3.1.5 Polymerase chain reaction (PCR)

Polymerase chain reaction (Saiki et al., 1985) was used to genotype the animals and to amplify cDNA fragments for cloning the *in situ* probes. Primers were designed using Oligo7 software (Molecular Biology Insights) and PCR was performed with Biometra thermal cyclers.

2.3.2 Genotyping

PCR conditions and program used for genotyping *Dll1^{LacZ}*, *Dll1^{Ki}*, *MyoD$^{-/-}$*, *Pax3^{Cre}* animals

1.5mM $MgCl_2$
3.5% DMSO
0.0935% β-mercaptoethanol
10µM of each primer
0.5mM dNTPs (Invitek)
12.5% sucrose
0.146% $(NH_4)_2SO_4$
0.0042% Cresol Red
0.125µl Taq polymerase (Invitrogen)

The program:

94°C - 4 min
95°C - 30 sec
55°C - 30 sec — 40x
72°C - 60 sec
72°C - 7 min
12°C

PCR conditions and program used for genotyping *Integrin-β1$^{flox/flox}$* animals

1.8mM $MgCl_2$
10µM of each primer
0.5mM dNTPs
0.2µl Taq polymerase

PCR Program:

94°C - 4 min
95°C - 30 sec
60°C - 30 sec — 35x
72°C - 60 sec
72°C - 4 min
12°C

PCR conditions and program used for genotyping *ILK$^{flox/flox}$* animals

1.5mM $MgCl_2$
10µM of each primer
0.5mM dNTPs
0.2µl Taq polymerase

PCR program:

95°C - 5 min
95°C - 30 sec
68°C - 30 sec — 8x
72°C - 30 sec
95°C - 30 sec
60°C - 30 sec — 40x
72°C - 30 sec
12°C

PCR conditions and program used for genotyping *Rosa*^{YFP} animals

1.8mM $MgCl_2$
10µM of each primer
0.5mM dNTPs
0.2µl Taq polymerase

PCR Program:

94°C - 4 min
95°C - 60 sec
60°C - 60 sec — 35x
72°C - 60 sec
72°C - 5 min
12°C

2.3.3 Quantitative polymerase chain reaction

qPCR was performed using 2x Absolute qPCR SYBR Green Mix (Thermo Scientific), 2µM primers and 1µl cDNA. Bio-Rad C1000 Thermal Cycler was used to amplify cDNA fragments.

Program used for qRT-PCR:

95°C - 15 min

95°C - 30 sec
60°C - 30 sec
72°C - 30 sec
} 40x

95°C to 65°C - 0.5°C/10 sec decrement (melting curve)

2.3.3.1 DNA amplification for generation of riboprobes for *in situ* hybridization

Specific DNA fragments of *Dll1* and *MyoR* gene were amplified from E12.5 whole embryo cDNA. PCR conditions were the same as for genotyping of the animals. The PCR product was cloned into pGEM-T Easy plasmid using T4 DNA ligase (Promega). Downstream primers contained T3 RNA polymerase promoter used to verify the sequence of PCR product by DNA Sequencing (Invitek) (AATTAACCCTCACTAAAGGG). Upstream primers were designed to contain XhoI restriction site (TCTGAG). XhoI enzyme (New England Biolabs) was used to linearize 10µg of plasmid at 37°C in 1h. *In vitro* transcription of the antisense probe was performed using DIG-RNA labeling kit (Roche). 500ng of plasmid was transcribed at 37°C in 2h. Labeled cRNA was purified using RNeasy clean-up kit (Qiagen) and eluted in 50µl H_20. The probes were stored in 50% formamide at -80°C.

2.3.4 Dissection and fixation of mouse tissue

The mouse heads were dissected in PBS and fixed in ice-cold 4% Zamboni's fixative for 2h. After several washings with ice-cold PBS the tissue was incubated overnight in 25% sucrose. The mouse heads were embedded in OCT compound (Sakura) and frozen on dry ice.

2.3.5 Preparation of frozen sections

Frozen tissue was cut in 12µm (for immunohistochemistry) and 16µm (for *in situ* hybridization) on a cryostat (Microtom HM560, Walldorf). The sections were collected on glass slides (Marienfeld) and dried for 2h at 37°C. The slides were stored at -80°C.

2.3.6 Immunohistochemistry

The slides were dried for 1h at 37°C. Unspecific binding of secondary antibodies was blocked by incubation for 1h at room temperature in TSA blocking solution. The slides were incubated with the primary antibodies diluted in staining buffer overnight at 4°C. After several washing steps in PBS containing 0.1% Triton X-100, the slides were incubated for 1h with secondary antibodies conjugated to Cy2, Cy3 or Cy5 and DAPI (Sigma-Aldrich) diluted in staining buffer. Following additional washings in PBS containing 0.1% Triton X-100, the slides were covered with Shandon Immu-Mount (Thermo Scientific).

For Pax7 staining, the slides were first incubated at 80°C for 20 min in Antigen Unmasking Solution (Vector Laboratories). The following steps of immunohistochemistry were performed as described above.

2.3.7 *In situ* hybridization

The cryosections were postfixed in cold 4% PFA for 10 min and washed 3 times in PBS. The slides were incubated for 10 min in acetylation buffer, washed 3 times in PBS and prehybridized for 2h at room temperature in hybridization buffer. DIG-labeled probes were diluted in hybridization buffer (1µl probe per 100µl) and denatured for 5 min at 80°C. The probe was added onto the slides and covered with coverslips. The hybridization was carried out overnight at 65°C in a humidified chamber. The slides were washed in 5x SSC for 5min, 0.2x SSC for 1h at 70°C, 0.2x SSC for 5 min at room temperature and B1 buffer for 5 min at room temperature. Blocking solution was added onto the slides for 1h at room temperature. The samples were incubated overnight at 4°C with AP-conjugated

anti-DIG Fab fragments (Roche) diluted 1:2,000 in blocking solution. The next day, the slides were washed 3 times for 5 min in B1 buffer and one time with NTMT. The slides were incubated at room temperature in *in situ* staining solution containing NBT and BCIP. After the signal was detected, the reaction was stopped by washes in water. The slides were air dried and covered with Shandon Immu-Mount (Thermo Scientific).

2.3.8 Whole mount *in situ* hybridization

Mouse embryos were dissected in ice-cold PBS and fixed overnight with 4% PFA. The next day, the embryos were washed 2 times for 10 min in PBS containing 0.1% Tween20 (PBT). Next the embryos were dehydrated by washing for 10 min in 50% methanol and 50% PBT. The embryos were collected in 100% methanol and stored at -20°C. After wild-type and mutant embryos were collected, the samples were rehydrated at 4°C by the following washing steps: 10 min 75% methanol/PBT, 10 min 50% methanol/PBT and 10 min 25% methanol/PBT. After 2 washes in PBT the embryos were bleached for 1h in 6% H_20_2. The embryos were washed 3 times at room temperature for 10 min in PBS and incubated in proteinase K buffer for 3 min. The following 5 min washing steps were performed: 2 times in PBT containing 2mg/ml glycine, 2 times in PBT, 3 times in RIPA-buffer and 3 times in PBT. Next the samples were fixed for 20 min in 4% PFA containing 25% glutaraldehyde and 10% Tween 20, and washed 3 times for 5 min in PBT, one time for 10 min in 1:1 solution of PBT and hybridization buffer for whole mount *in situ*, and 10 min in hybridization buffer. The embryos were prehybridized at 65°C for 1h in hybridization buffer. 10µl DIG-labeled *in situ* probe and 10µl 10mg/ml tRNA were diluted in 1ml of hybridization buffer, denatured at 80°C for 5 min and cooled on ice. The probe was incubated with the embryos overnight at 65°C. The next day, the samples were washed at 65°C two times in hybridization buffer for 30 min, one time in 1:1 solution of hybridization buffer and SSC/FA/T for 10 min, 5 times for 10 min in SSC/FA/T and 6 times for 20 min in SSC/FA/T. Next the embryos were washed at room temperature for 10 min with 1:1 solution of hybridization buffer and SSC/FA/T and 2 times for 10 min

in MABT. After blocking for 1h in 5% Roche blocking buffer in MABT, AP-conjugated anti-DIG Fab fragments (Roche) diluted in 1% Roche blocking buffer were incubated overnight with the embryos. The next day, the embryos were washed 10 times for 30 min in PBT containing 2mM tetramisole hydrochloride and the last wash was performed overnight at 4°C. On the last day, the embryos were washed 3 times for 30 min in alkaline phosphatase buffer. Signal was detected after the embryos were incubated in the dark in 1.5ml NTMT buffer containing 1.5µl of NBT and BCIP. When the signal reached required intensity, the reaction was stopped by washing the embryos in alkaline phosphatase buffer and transferring them to fixing solution. The embryos were stored in the dark at 4°C.

2.3.9 Isolation of satellite cells

Limb, tongue, cheek (masseter) and extraocular muscles from 4-week-old wild-type mice were dissected, minced and dissociated for 80 min at 37°C using NB4 collagenase (Serva, 0.3mg/ml), Dispase II (Roche, 2.5U/ml) and trypsin (Gibco, 0.008%, 5min, RT) in dissection medium. The tissue was filtered through 100µm, 70µm and 40µm strainers (Partec). An unconjugated Vcam-1 antibody (R&D Systems) combined with a DyLight488-conjugated secondary antibody (Dianova) stained satellite cells. Bone marrow cells, endothelial cells and hematopoietic cells were stained using APC-conjugated antibodies against Sca-1, CD31 and CD45 (BD Biosciences). All antibodies were dissolved in the staining buffer. Dead cells were marked using propidium iodide (Invitrogen). Satellite cells ($VCAM^+$/$Sca\text{-}1^-$,$CD31^-$,$CD45^-$) were isolated using BD FACS Aria II sorter (BD Biosciences) and collected in TRIzol reagent (Ambion). The purity of the isolated cells was defined by Pax7 immunohistology. 80%-85% of the sorted cytospun cells were Pax7+.

2.3.10 Preparation of myoblasts and muscle fibers

2.3.10.1 Myoblast fusion assay

The forelimbs and hindlimbs of E14.5 embryos were dissected in 1x PBS and minced using a scalpel. The tissue was transferred to a 1.5ml tube containing 200µl HBSS (+Mg^{2+} and Ca^{2+}) and 1:40 NB4 collagenase (6mg/ml). The tissue was incubated at 37°C for 40 minutes. The digestion reaction was stopped by adding 500µl medium (DMEM + 4.5g/l glucose, 10% FCS, 1% gentamicin) and filtered through a 20µm filter (Partec) to obtain single cell suspension. The cells were spun for 5 min at 2000 rpm and the cell pellet was resuspended in 100µl medium. The cells were plated onto two wells of a 12-well culture plate containing glass coverslips coated with 40µg/ml Poly-L-Lysine. The cells were cultured over night in the medium containing 10% FCS. The day after the medium was changed to DMEM + 4.5g/l glucose, 5% FCS, 1% gentamicin and cultured for 72h. The cells were fixed for 10 minutes with 4% PFA, washed 3 times with 1x PBS and stored at 4°C.

2.3.10.2 Isolation of muscle fibers

The skin from the forelimbs of E18 embryos was removed using thin forceps. The limbs were transferred into a 2ml tube containing 1ml medium (DMEM + 4.5g/l glucose, 20mM HEPES, 1% gentamicin) and 1:20 NB4 collagenase (6mg/ml). The digestion reaction was carried out at 37°C and rotated at 100 rpm for 1h. The cells and fibers were plated onto two wells of a 12-well culture plate containing glass coverslips coated with 40µg/ml Poly-L-Lysine. The medium containing 10% FCS was added to the wells. The cells were fixed 16h later with 4% PFA for 20 min, washed 3 times with 1x PBS and stored at 4°C.

2.3.11 Data analysis

2.3.11.1 Documentation of histological data

The histological data was documented using Laser Scanning Microscope LSM700 and Axio Observer Z1 Microscope and Zen software (Zeiss).

2.3.11.2 Quantifications and statistical analysis

Cell counts were performed on muscle tissue of three or more animals of each genotype. The statistical significance was determined using unpaired Student's two-tailed t-test in Microsoft Excel software.

Fusion index was calculated as a ratio of the number of nuclei inside myotubes to the number of total nuclei x 100. Average and standard error of the mean were displayed on the graphs.

3 Results

3.1 Expression of the Notch ligand Dll1 in craniofacial muscles during development

Trunk myogenesis is repressed by Notch signaling through suppression of MyoD. To examine the role of Notch signaling during head myogenesis, I analyzed components of the Notch signaling cascade in head muscle. First, I defined expression of *Dll1* at an early developmental stage when myogenic progenitor cells reach their positions in the head and begin to form craniofacial muscles. *In situ* hybridization showed that *Dll1* is expressed at E11.5 in developing muscle of the tongue, in pharyngeal arch-derived muscle in the cheek and in extraocular muscle (Fig. 1A). To confirm that the *Dll1* signal is located indeed in muscle tissue, a consecutive section was stained with an antibody directed against desmin (Fig. 1B).

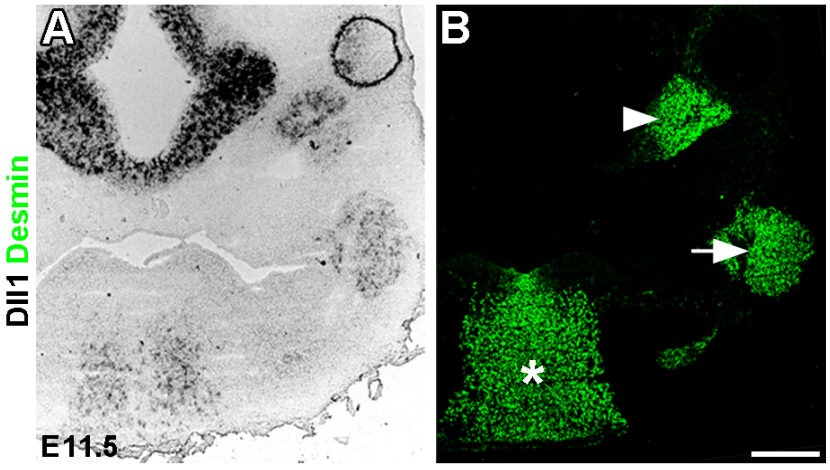

Figure 1. ***Dll1* expression in craniofacial muscles**
(A) *In situ* hybridization using a *Dll1*-specific probe demonstrates the expression of *Dll1* in the developing craniofacial muscle at E11.5. (B) Anti-desmin

immunohistology was used to define the exact location of craniofacial muscle groups. Branchiomeric muscle (arrow), extraocular muscle (arrow head), and tongue muscle (asterisk) are indicated. Scale bar: 300 µm.

To compare expression of *Dll1* in different muscle groups, I isolated mRNA from the *tibialis anterior*, masseter, tongue and extraocular muscle from E18 and P21 mice. Using quantitative PCR analysis, I showed that expression of *Dll1* was comparable in all tested muscle groups (Fig. 2)

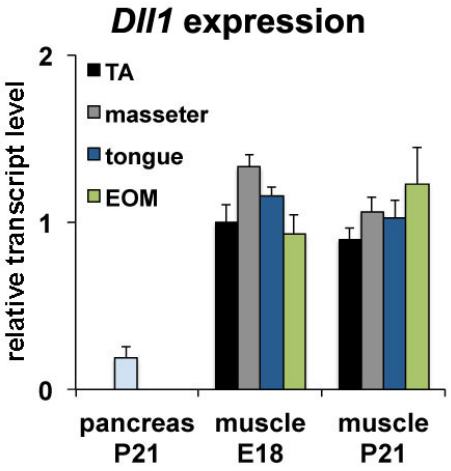

Figure 2. ***Dll1* expression in the muscles of prenatal and adult mice**
Quantification of *Dll1* mRNA isolated from *tibialis anterior* (black), masseter (grey), tongue (blue) and extraocular muscle (green) at E18 and P21 by qRT-PCR. mRNA isolated from P21 pancreas was used as a negative control. Error bars, SEM.

3.2 Expression of Notch signaling molecules in craniofacial muscles

To define the expression of various Notch signaling molecules in myogenic progenitors, I isolated satellite cells from 4-week-old mice. Tongue, masseter, extraocular muscles and muscles of the limbs were dissected, dissociated and filtered through 100 µm, 70 µm and 40 µm strainers to obtain single cell

suspensions. The cells were stained with an anti-Vcam-1 antibody marking the satellite cells. Additionally, antibodies directed against Sca-1, CD31 and CD45 were used to stain bone marrow cells, endothelial cells and hematopoietic cells. Propidium iodide (PI) was used to mark dead cells, to exclude them from the sorted fraction. Cells positive for Vcam-1 and negative for Sca-1, CD31, CD45 and propidium iodide were isolated using fluorescence-activated cell sorting (FACS) (Fig. 3).

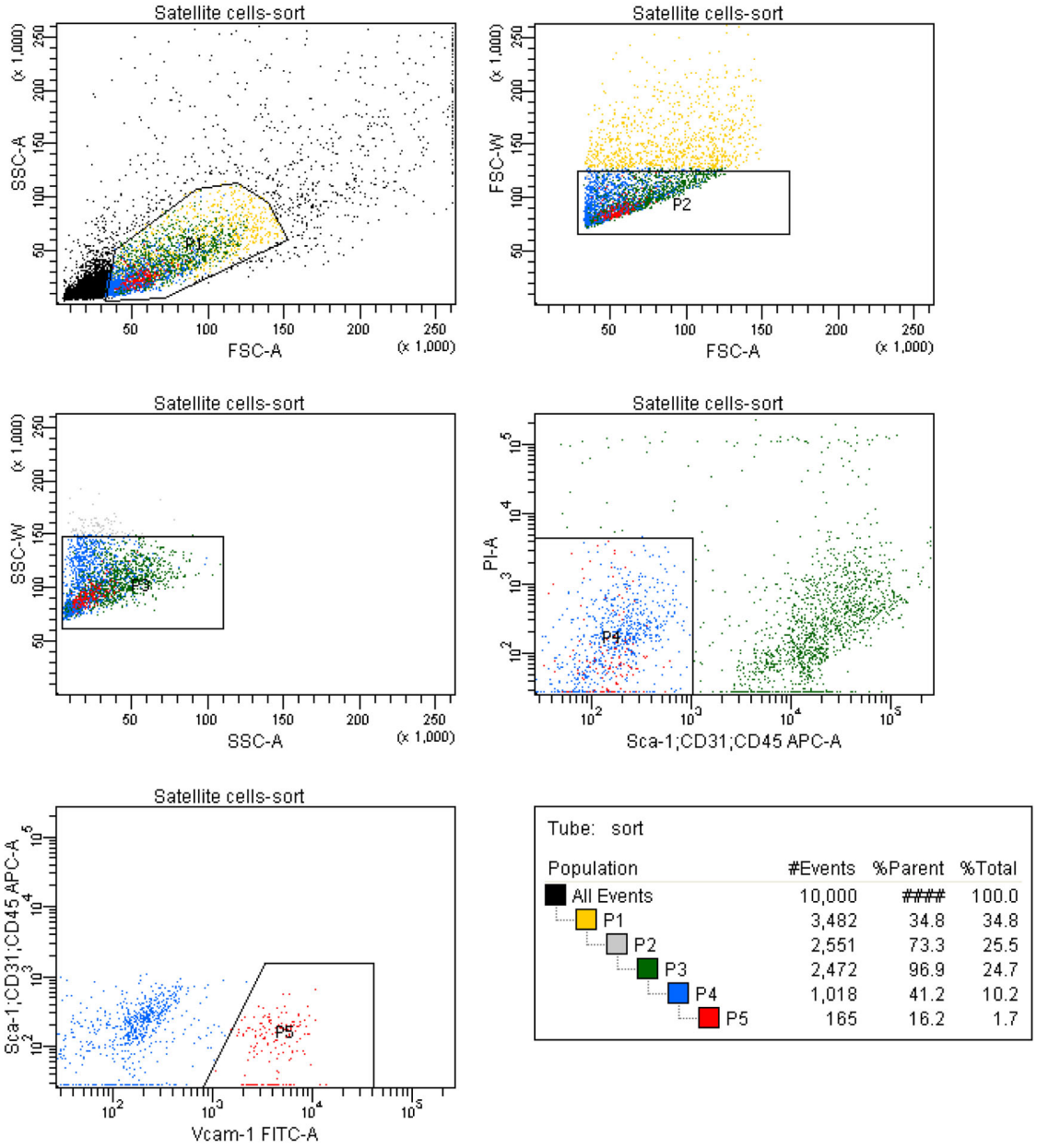

Figure 3. **Gating strategy used to isolate satellite cells by FACS**
The gates used to isolate progenitor cells and the number of events contained in each gate is shown. The cells were stained with APC-conjugated antibodies directed against Sca-1, CD31, CD45 and an anti-Vcam-1 antibody combined with a DyLight488-conjugated secondary antibody. Dead cells and debris were excluded by PI-staining and by gating on forward and side scatter profiles. Cells in population P5 (Vcam-1+, Sca-1-/CD31-/CD45-) were collected.

To define the identity and purity of the sorted cells, they were cytospun onto adhesive glass slides and stained with antibodies directed against Pax7 and MyoD (Fig. 4). 85-90% of the FACS-isolated cells were Pax7-positive, and only a small subpopulation co-expressed Pax7 and MyoD.

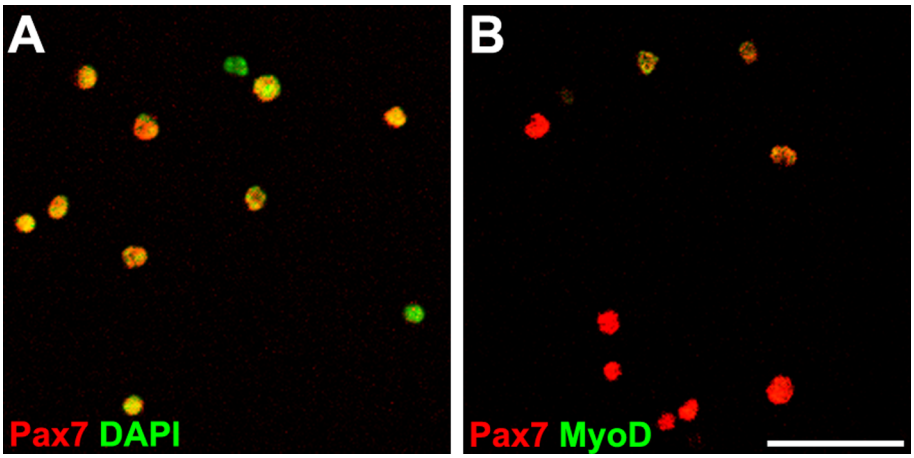

Figure 4. **Purity of FACS-isolated cells**
Immunohistological analysis of sorted satellite cells that were cytospun after isolation and stained by immunohistology using anti-Pax7 and anti-MyoD antibodies as indicated. Nuclei were counterstained with DAPI. Scale bar: 50 µm.

Total RNA was isolated from the freshly sorted satellite cells of the limb, masseter, tongue and extraocular muscles. First strand DNA was synthesized and used as a template for quantitative PCR. Components of the Notch signaling pathway and direct Notch target genes were amplified with specific oligonucleotides. Expression levels of *Notch1, Notch3, Rbpj, Hey1, Dll1, Hes1* and *Pax7* in masseter, tongue and extraocular muscle were compared to the levels observed in satellite cells from limb muscle. The *Notch1/3* receptors, *Rbpj*

and the Notch target gene *Hey1* were expressed at comparable levels in satellite cells independent of their muscle of origin (Fig. 5). The Notch ligand *Dll1* and the Notch target gene *Hes1* were expressed at higher levels in masseter and tongue muscle than in leg and extraocular muscle. Overall, the expression analysis in satellite cells indicates that the Notch signaling pathway is active in craniofacial muscles of the adult mice.

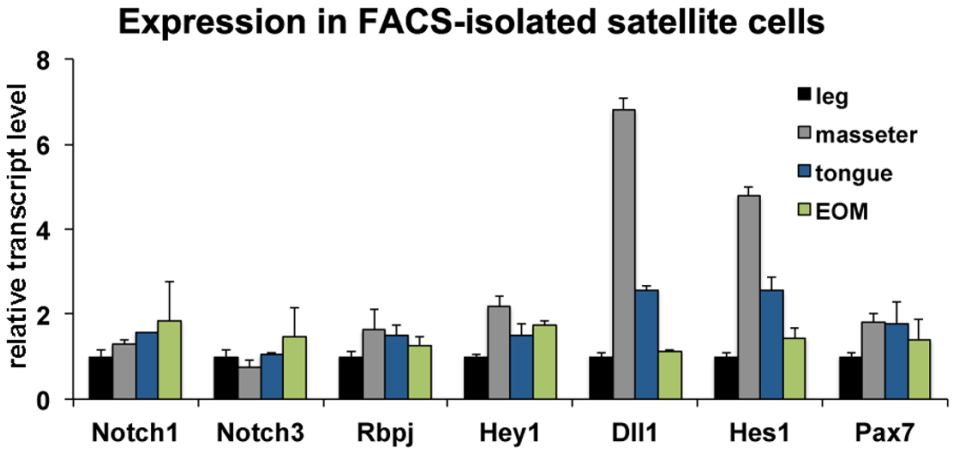

Figure 5. **Expression of Notch signaling molecules in craniofacial muscles** qRT-PCR analysis of various components of the Notch signaling pathway in FACS-isolated satellite cells from different muscle groups. Gene expression levels in satellite cells from masseter (grey), tongue (blue) and extraocular muscle (green) relative to expression levels in satellite cells from leg muscle (black) are shown. Error bars, SEM.

3.3 *Dll1* mutation in skeletal muscles

A strong hypomorph *Dll1* mutation ($Dll1^{LacZ/Ki}$) was previously shown to cause premature myogenic differentiation, resulting in the depletion of the myogenic progenitor pool and a severe reduction of the muscle mass (Schuster-Gossler et al., 2007). Dominique Bröhl in the laboratory had also performed immunohistological analyses of the distal forelimb of $Dll1^{LacZ/Ki}$ mutant mice at E17.5, which had revealed that only tiny muscle groups were formed (Fig. 6).

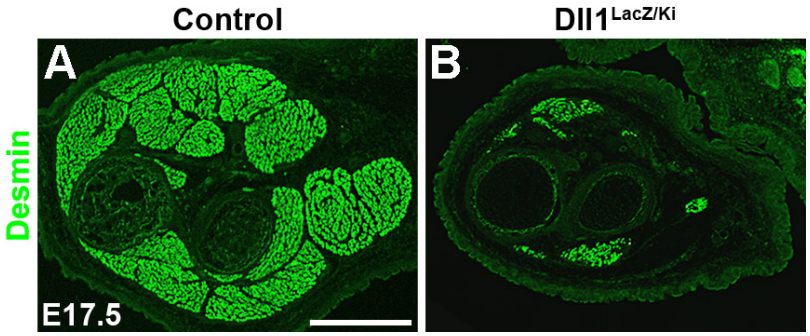

Figure 6. ***Dll1* mutation leads to the formation of tiny muscle groups**
Immunohistological analysis of limb muscle at E17.5 in control (A) and *Dll1*$^{LacZ/Ki}$ (B) mice. The muscle was visualized using antibodies directed against desmin. Scale bar: 500 µm. Adapted from Bröhl et al., 2012.

3.4 Mutation of *Dll1* results in formation of tiny muscle groups in the head

In the developing muscle, a pool of myogenic progenitor cells is formed and maintained. These resident progenitors provide a source of cells for muscle growth. To investigate the role of *Dll1* in the development of craniofacial muscles, embryonic heads of E13 control and *Dll1*$^{LacZ/Ki}$ mutant mice were dissected. The myogenic progenitor cells were visualized using an anti-Pax7 antibody. The sections were additionally stained with an antibody directed against myosin marking craniofacial muscles (Fig. 7).

Mutation of *Dll1* led to a strong reduction in the size of the masseter, whereas the size of tongue and extraocular muscles were little affected at this stage (Fig. 7B, B'). However, Pax7+ progenitor cells were absent in all cranial muscles.

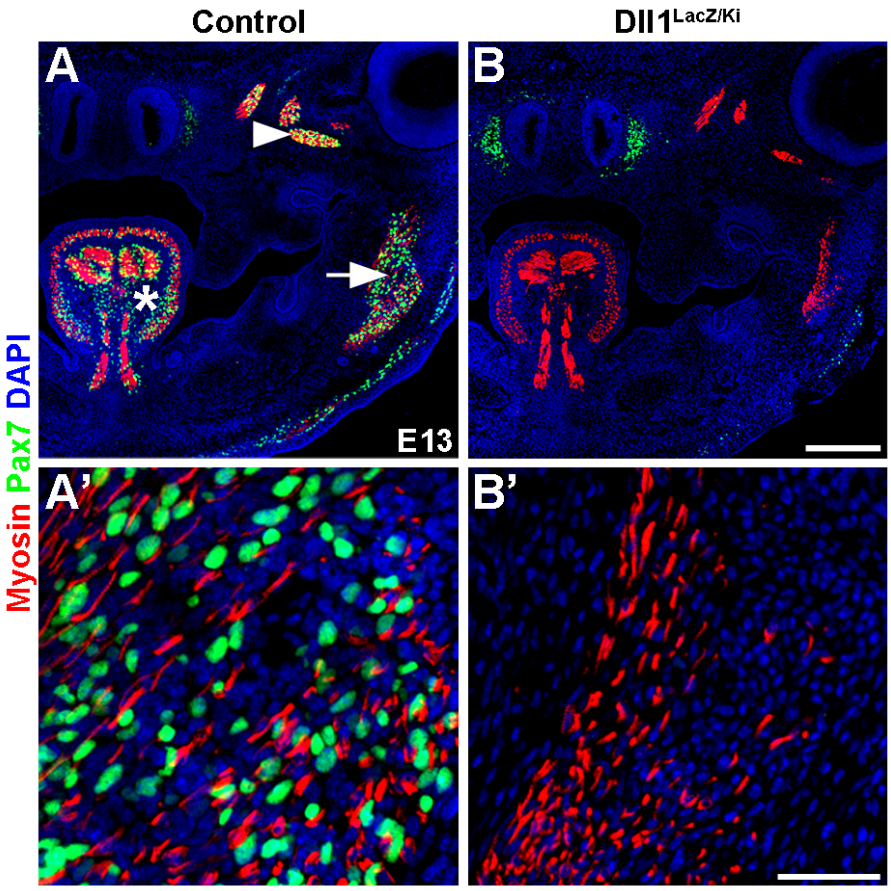

Figure 7. **Loss of Pax7+ progenitors in *Dll1* mutant embryos**
Immunohistological analysis of control (A) and *Dll1*$^{lacZ/Ki}$ mutant (B) mice at E13 revealed decrease in muscle size and a loss of Pax7+ progenitors; muscle and myogenic progenitor cells in the head were visualized by anti-myosin (red) and anti-Pax7 (green) antibodies. DAPI (blue) was used as a counterstain. (A', B') Higher magnification of masseter muscle. Arrow, arrowhead and asterisk indicate masseter, extraocular and tongue muscle, respectively. Scale bars: 300 µm in (A, B), 50 µm in (A', B').

At E18.5, a strong reduction of the shoulder and body wall muscles is observed in *Dll1*$^{LacZ/Ki}$ mice (Schuster-Gossler et al., 2007). I investigated whether, despite a different origin of craniofacial muscles, lack of the Notch ligand Dll1 leads to muscle defects in the head. At E18, sections of control (Fig. 8A) and *Dll1*$^{LacZ/Ki}$ mutant animals (Fig. 8B) were stained with antibodies marking myogenic progenitor cells (anti-Pax7) and differentiated myotubes (anti-myosin). *Dll1*

mutation resulted in premature differentiation of myogenic progenitors and pronounced reduction of the muscle size. The masseter and buccinator muscles derived from first and second branchial arch, respectively, as well as extraocular muscles were tiny in *Dll1*$^{LacZ/Ki}$ mutant animals (Fig. 8B). The size of tongue muscle that is of mixed origin and derives from somites and head mesenchyme was decreased but less strongly affected than other muscle groups. Pax7+ myogenic progenitor cells were absent in all craniofacial muscles of *Dll1*$^{LacZ/Ki}$ mutant mice, but were detectable in control mice.

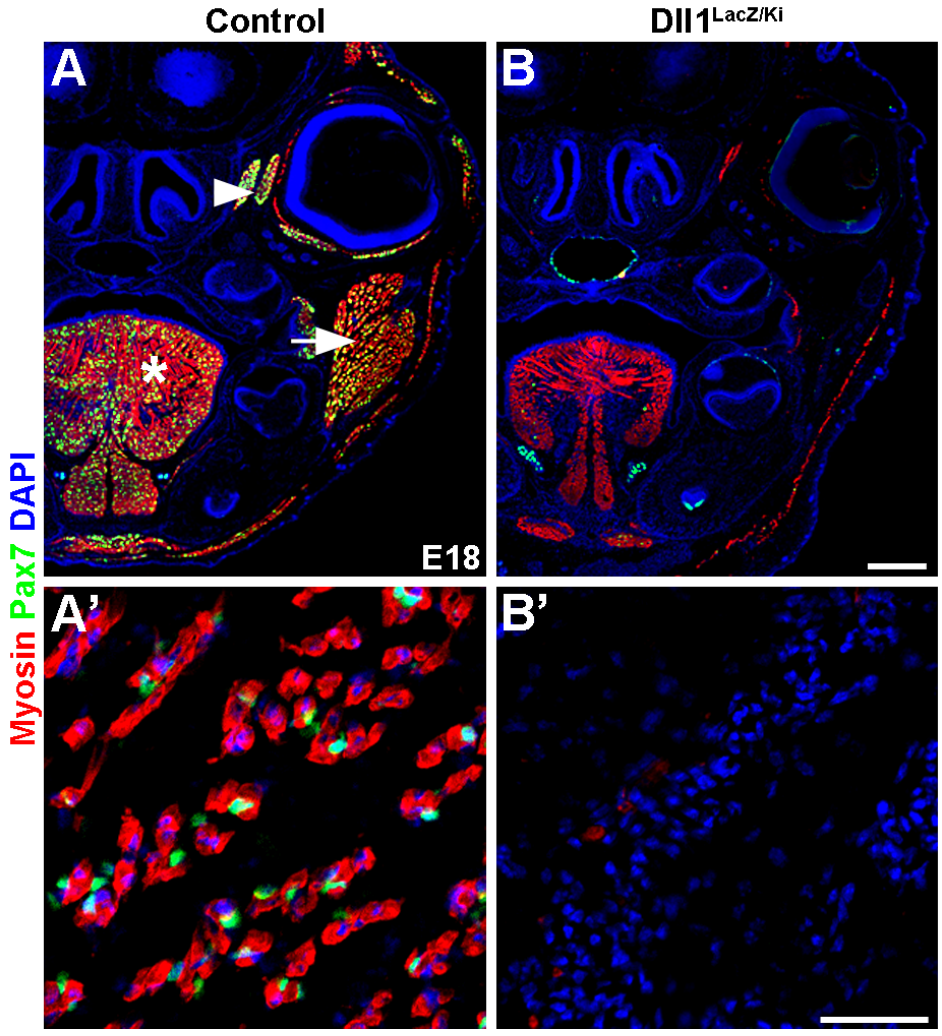

Figure 8. **Disrupted muscle growth and loss of Pax7+ progenitors in craniofacial muscle of *Dll1* mutants**
Immunohistological analysis of control (A) and *Dll1*$^{lacZ/Ki}$ mutant (B) mice at E18 revealed a pronounced decrease in muscle size and a loss of Pax7+ progenitors;

muscle and myogenic progenitor cells in the head were visualized by anti-myosin (red) and anti-Pax7 (green) antibodies. DAPI (blue) was used as a counterstain. (A', B') Higher magnification of masseter muscle. Arrow, arrowhead and asterisk indicate masseter, extraocular and tongue muscle, respectively. Scale bars: 300 µm in (A, B), 50 µm in (A', B').

3.5 Premature differentiation of craniofacial muscle progenitor cells in *Dll1* mutant mice

Loss of Notch signal in trunk muscles results in uncontrolled myogenic differentiation at early stages indicated by increased numbers of MyoD- and desmin-positive cells (Schuster-Gossler et al., 2007; Vasyutina et al., 2007). This results in a lack of muscle growth and severe muscle dystrophy.

I examined whether premature differentiation of myogenic progenitor cells could be observed in craniofacial muscles of $Dll1^{LacZ/Ki}$ mutant mice. Sections of E10.5 and E11.5 heads were stained with antibodies against MyoD, desmin and MyoG. The myogenic differentiation factor MyoD is one of the earliest markers of myogenic commitment and is expressed in proliferating and postmitotic myoblasts. I observed upregulated MyoD expression in the branchial arches at E10.5 in $Dll1^{LacZ/Ki}$ mutants compared to control mice (Fig. 9A, B). Quantification demonstrated that the number of MyoD+ nuclei in the desmin+ branchiomeric muscle area was increased in $Dll1^{LacZ/Ki}$ mutants compared to control animals (Fig. 9C). In addition, the MyoD signal was notably increased, i.e. MyoD protein was present at higher levels in nuclei of mutant myoblasts and more nuclei expressed MyoD (Fig. 9B). The expression of desmin, marking differentiating myoblasts and myotubes, was slightly increased in $Dll1^{LacZ/Ki}$ mutants.

In addition, MyoG expression, marking differentiated myotubes, was upregulated at E11.5 in craniofacial muscles of $Dll1^{LacZ/Ki}$ mutants (Fig. 9D, E). The numbers of MyoG+ nuclei as well as MyoG and desmin protein levels were increased (Fig. 9F). Thus, mutation of *Dll1* results in a broadened and premature differentiation of myogenic progenitors in craniofacial muscle.

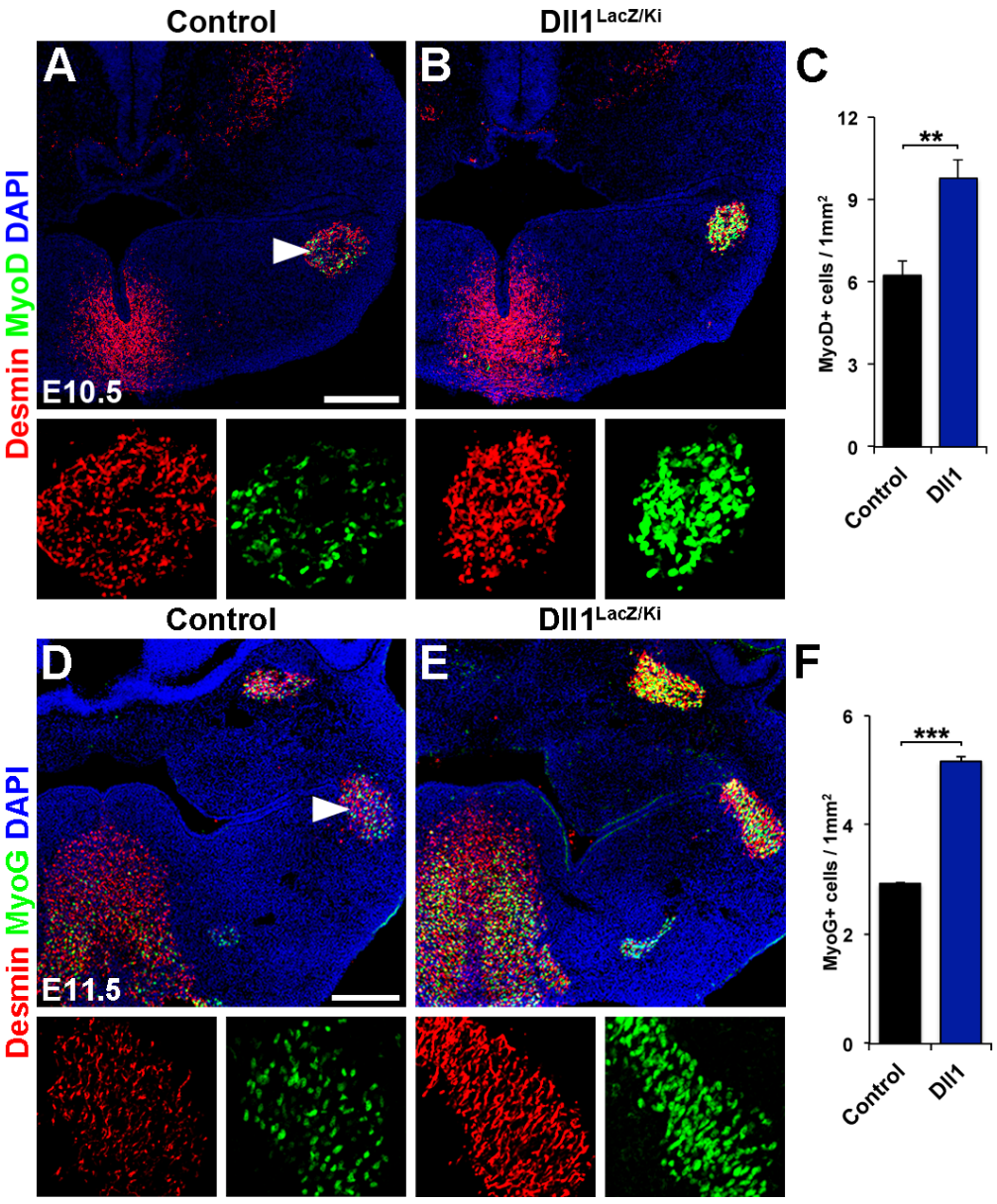

Figure 9. **Upregulated expression of myogenic regulatory factors in craniofacial muscle**
(A, B) Immunohistological analysis of craniofacial muscles in E10.5 control and *Dll1*$^{lacZ/Ki}$ mice using DAPI (blue) and antibodies against desmin (red) and MyoD (green). (C) Quantification of MyoD+ cells/1mm^2 in branchiomeric muscle. (D, E) Immunohistological analysis of control and *Dll1*$^{lacZ/Ki}$ mice at E11.5 using DAPI (blue) and antibodies against desmin (red) and MyoG (green). (F) Quantification of MyoG+ cells/1mm^2 in branchiomeric muscle. Error bars, SEM. Statistical significance is indicated (**p < 0.01; ***p < 0.001). Scale bars: 200 µm in (A, D).

3.6 *MyoR* expression is regulated by Notch signaling

The transcription factor MyoR regulates craniofacial myogenesis, and its expression is controlled by Notch signaling (Lu et al., 2002; Buas et al., 2009). I examined *MyoR* expression in head muscle of *Dll1*$^{LacZ/Ki}$ mutant animals by *in situ* hybridization.

At E11, *MyoR* was expressed in somites, branchial arches and limbs of control animals (Fig. 10A), and was strongly downregulated in *Dll1*$^{LacZ/Ki}$ mutants (Fig. 10B). At E11.5, the differences in *MyoR* expression were even more pronounced in somites and branchial arches, but signals in limb muscle appeared unchanged. In addition, the expression of *Pitx2*, *Tbx1* and *Myf5* that drive myogenesis in head muscles were also unaffected (Fig. 11). I conclude that mutation of *Dll1* results in a broadened differentiation of head muscle, upregulated MyoD and MyoG protein expression, which is accompanied by decreased expression of *MyoR*.

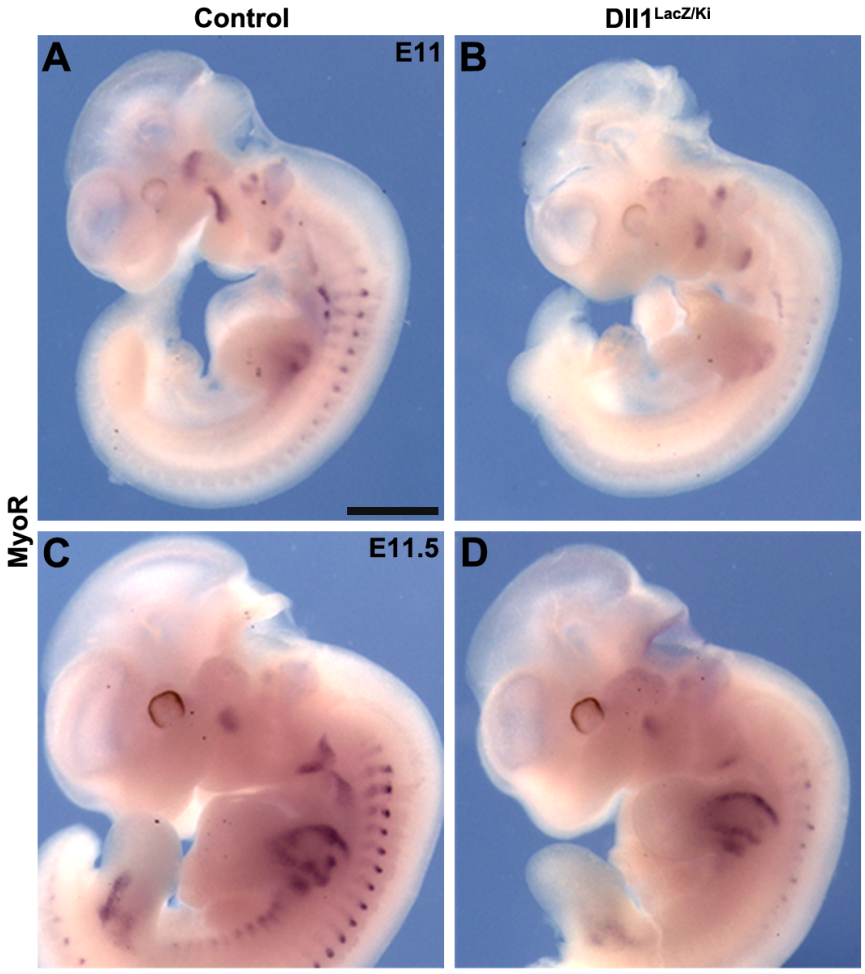

Figure 10. **Downregulation of *MyoR* in *Dll1* mutant animals**
Whole-mount *in situ* hybridization using a *MyoR*-specific probe on control and *Dll1*$^{LacZ/Ki}$ mice at E11 (A, B) and E11.5 (C, D). Scale bar: 1mm.

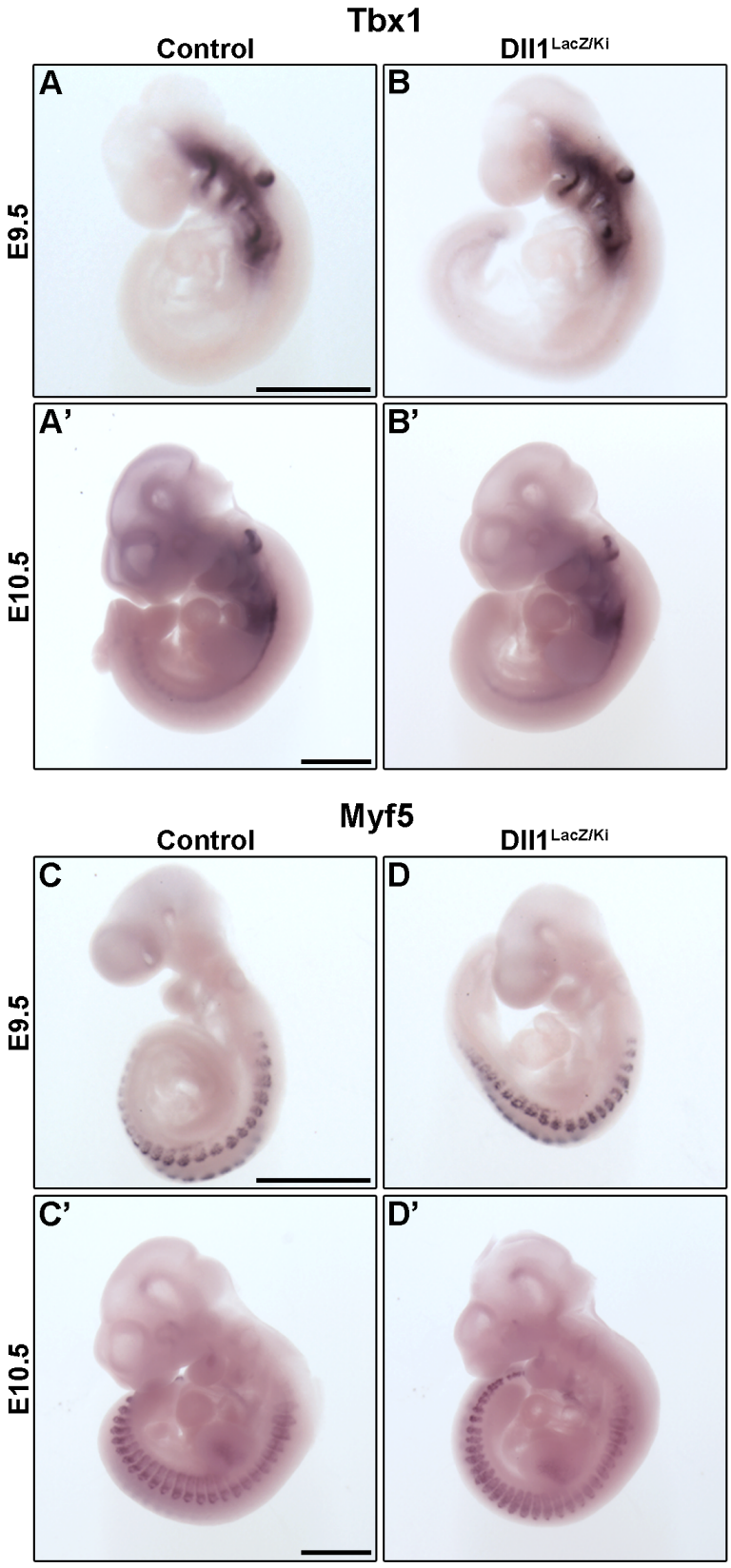
Tbx1
Control
Dll1LacZ/Ki
A
B
E9.5
A'
B'
E10.5
Myf5
Control
Dll1LacZ/Ki
C
D
E9.5
C'
D'
E10.5

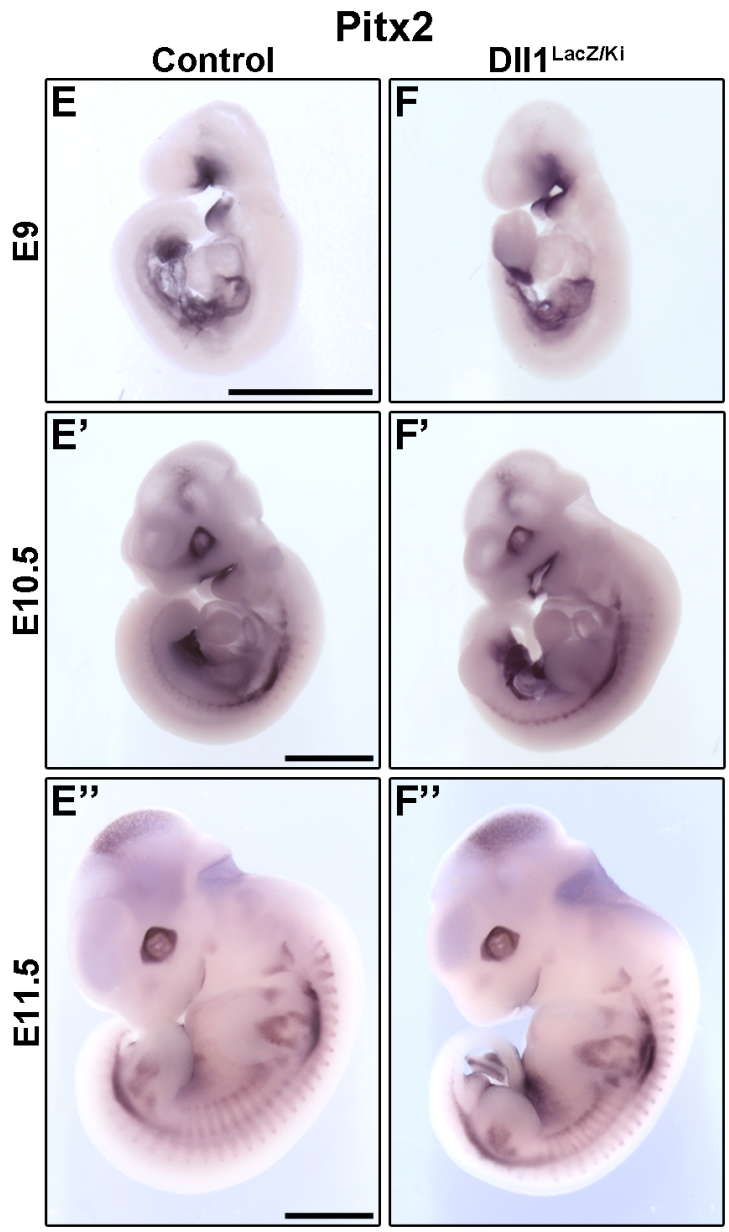

Figure 11. **The expression of *Tbx1*, *Myf5* and *Pitx2* is not affected in *Dll1* mutant embryos**
Whole-mount *in situ* hybridization using *Tbx1* (A, B), *Myf5* (C, D) and *Pitx2*-specific (E, F) probes on control and *Dll1*$^{LacZ/Ki}$ mutant mice at indicated developmental stages. Scale bars: 1mm.

3.7 Mutation of *MyoD* rescues the myogenic stem cell pool in *Dll1* mutants

We recently showed that the deficits in trunk muscle growth that are caused by mutation of Notch signaling components are rescued by ablation of *MyoD* (Bröhl et al., 2012). I therefore analyzed craniofacial muscle of *Dll1*$^{LacZ/Ki}$;*MyoD*$^{-/-}$ double mutants. Compared to *Dll1*$^{LacZ/Ki}$ mice (Figure 12A), the size of craniofacial muscle groups was markedly increased in *Dll1*$^{LacZ/Ki}$;*MyoD*$^{-/-}$ mutants (Figure 12B). Overall structure and size of craniofacial muscles were comparable in *Dll1*$^{LacZ/Ki}$;*MyoD*$^{-/-}$ and *MyoD*$^{-/-}$ mutants, and in particular both the extrinsic and intrinsic tongue muscle mass was increased. Remarkably, in the *Dll1*$^{LacZ/Ki}$;*MyoD*$^{-/-}$ mutant mice the number of Pax7+ myogenic progenitor cells in the extrinsic part of the tongue was comparable to *MyoD*$^{-/-}$ mutants but Pax7+ progenitor cells in the intrinsic tongue were rare (Figure 12B, C). Thus, the introduction of the *MyoD* mutation rescues the deficit in the craniofacial muscle size caused by mutation of *Dll1*, and allows Pax7+ progenitor cells to be maintained in all head muscle with the exception of the intrinsic tongue muscle. In addition, *MyoR* expression was not restored (Fig. 13).

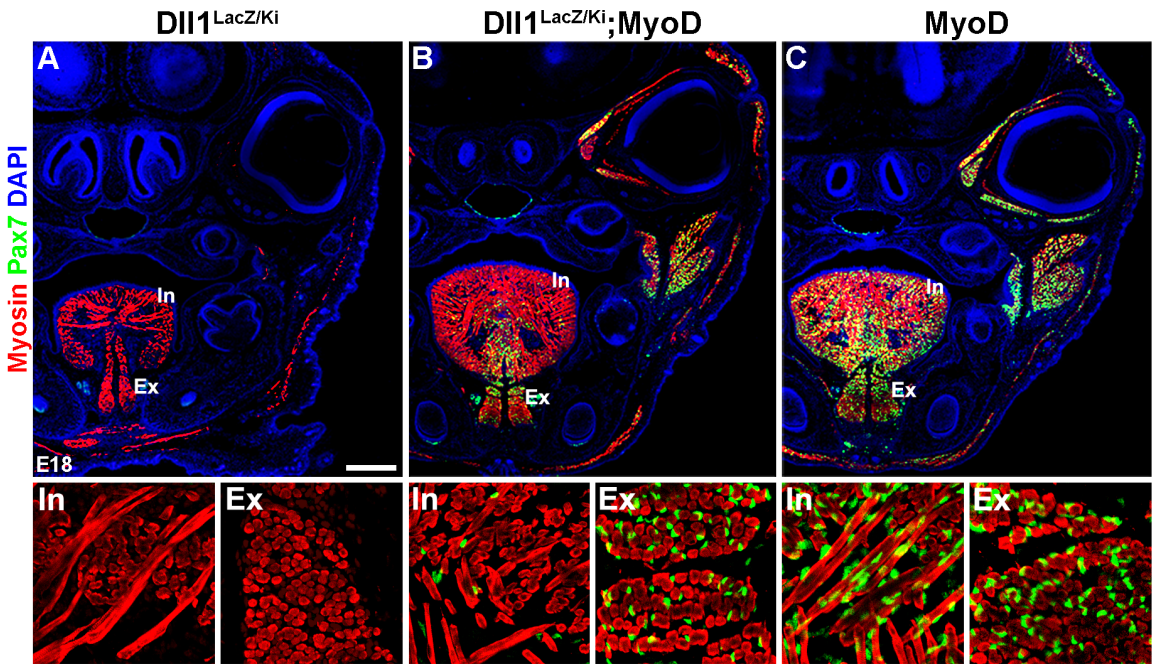

Figure 12. **MyoD-dependent rescue of myogenic progenitors in *Dll1* mutant mice**

Immunohistological analysis of craniofacial muscle in *Dll1*$^{lacZ/Ki}$ (A), *Dll1*$^{lacZ/Ki}$*;MyoD*$^{-/-}$ (B) and *MyoD*$^{-/-}$ (C) mice at E18 using DAPI (blue) and antibodies against myosin (red) and Pax7 (green). Note the marked increase in the size of the muscle in *Dll1*$^{lacZ/Ki}$*;MyoD*$^{-/-}$ compared to *Dll1*$^{lacZ/Ki}$ mice. In - intrinsic part of the tongue, Ex - extrinsic part of the tongue. Scale bar: 500 µm.

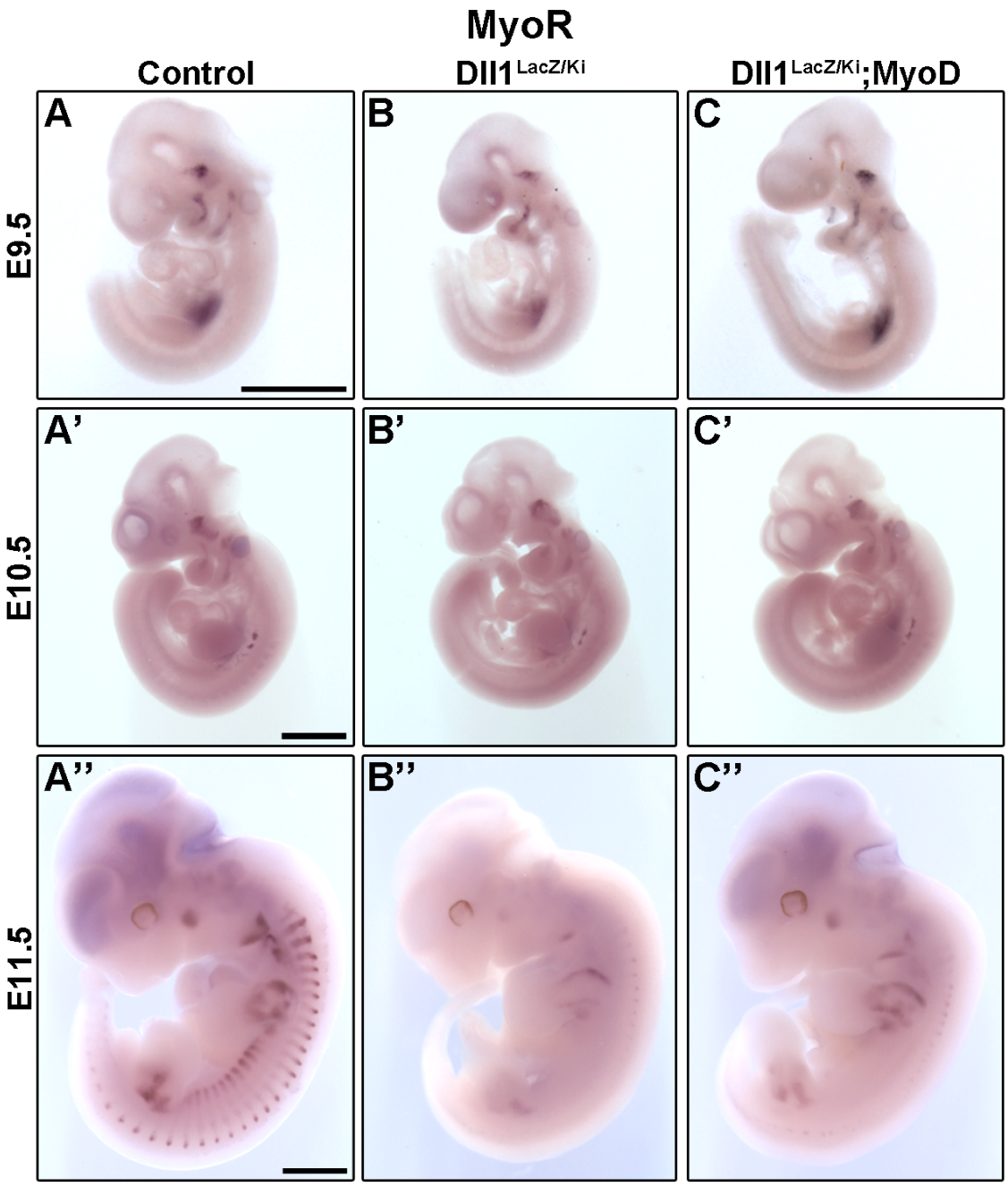

Figure 13. **The expression of *MyoR* is not restored in *Dll1$^{lacZ/Ki}$;MyoD$^{-/-}$* double mutant animals**
Whole-mount *in situ* hybridization using a *MyoR*-specific probe on control, *Dll1$^{LacZ/Ki}$* and *Dll1$^{lacZ/Ki}$;MyoD$^{-/-}$* mutant mice at E9.5 (A-C), E10.5 (A'-C') and E11.5 (A"-C"). Scale bars: 1mm.

I also analyzed the number of Pax7+ progenitor cells associated with craniofacial muscle in *MyoD*-rescued *Dll1* mutants. The sections of E18 animals were stained using antibodies directed against myosin marking muscles and anti-Pax7 antibodies detecting myogenic progenitors (Fig. 14). Whereas Pax7+ cells were absent in all craniofacial muscles of *Dll1*$^{LacZ/Ki}$ mutant mice (Fig. 14B), their number was markedly increased in *Dll1*$^{LacZ/Ki}$*;MyoD*$^{-/-}$ double mutant mice (Fig. 14C). It should be noted that craniofacial muscles of *MyoD*$^{-/-}$ mutants contain supernumerary progenitor cells (Fig. 14D). The numbers of Pax7+ progenitor cells in the *Dll1*$^{LacZ/Ki}$*;MyoD*$^{-/-}$ and *MyoD*$^{-/-}$ mutants reached comparable levels in masseter and extrinsic tongue muscles (Fig. 14E, E'). I also observed a rescue of progenitor cells in extraocular muscles, but the rescue was less pronounced, i.e. the number of Pax7+ cells in *Dll1*$^{LacZ/Ki}$*;MyoD*$^{-/-}$ were lower that in *MyoD*$^{-/-}$ mice (Fig. 14E''). In conclusion, deficits in muscle size and in the progenitors pools that are caused by mutation of *Dll1* in craniofacial muscle are substantially rescued by *MyoD* mutation.

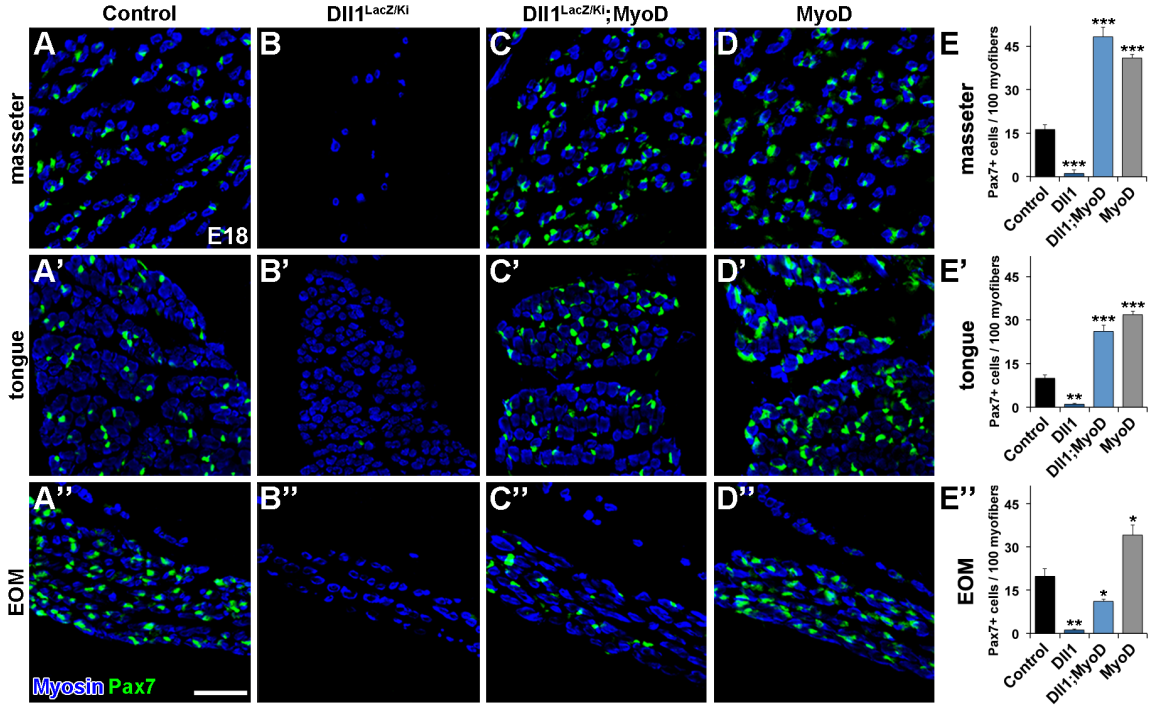

Figure 14. **Loss of myogenic progenitor cells in *Dll1* mutant mice and rescue upon *MyoD* ablation**
(A-D) Analysis of numbers of Pax7+ cells (green) in masseter, tongue and extraocular muscle at E18 of control (A), *Dll1*$^{LacZ/Ki}$ (B), *Dll1*$^{LacZ/Ki}$;*MyoD*$^{-/-}$ (C) and *MyoD*$^{-/-}$ (D) mutant animals. **(E-E'')** Quantification of Pax7+ cells/100 myofibers. Error bars, SEM. Statistical significance is indicated (*p < 0.05; **p < 0.01; ***p < 0.001). Scale bars: 50 µm.

3.8 Homing of emerging satellite cells in craniofacial muscle

Satellite cells are wedged between the basal lamina and plasma membrane of myofibers (Mauro, 1961). They emerge around E15.5, when a basal lamina forms around myofibers (Gros et al., 2005; Kassar-Duchossoy et al., 2005; Relaix et al., 2005). In the trunk, the majority of Pax7+ cells locate to the interstitial space in *Dll1*$^{LacZ/Ki}$;*MyoD*$^{-/-}$ mutants, indicating that emerging satellite cells cannot home correctly (Bröhl et al., 2012). To investigate whether Notch participates in satellite cell homing in craniofacial muscles, I analyzed the localization of myogenic progenitor cells. Cryosections of E18 mice were stained using an antibody directed against laminin, marking the basal lamina of the muscle fibers, and an anti-Pax7 antibody indicating myogenic progenitor cells (Fig. 15). I quantified the number of Pax7-positive myogenic progenitor cells (number of cells/100 fibers) localized below the basal lamina (Fig. 15E). In control animals at E18, the majority of muscle progenitor cells were located below the basal lamina (87%, 85% and 80% in the masseter, extrinsic part of tongue and EOM, respectively), and the remainder resided in the interstitial space (Fig. 15A). In *MyoD*$^{-/-}$ mutants, the overall numbers of Pax7+ cells were increased, and many of the supernumerous cells located to the interstitial space (Figure 15C, F). Thus, the proportion of cells below the lamina was decreased (63%, 65% and 69% in the masseter, extrinsic tongue muscle and EOM, respectively). In *Dll1*$^{LacZ/Ki}$;*MyoD*$^{-/-}$ double mutant mice, very moderate changes in the proportion of cells located below the lamina were observed (63%, 51% and 45% in the masseter, extrinsic part of tongue and EOM, respectively; Figure 15D,

F). Thus, Notch signaling impinges little on satellite cell homing in craniofacial muscle.

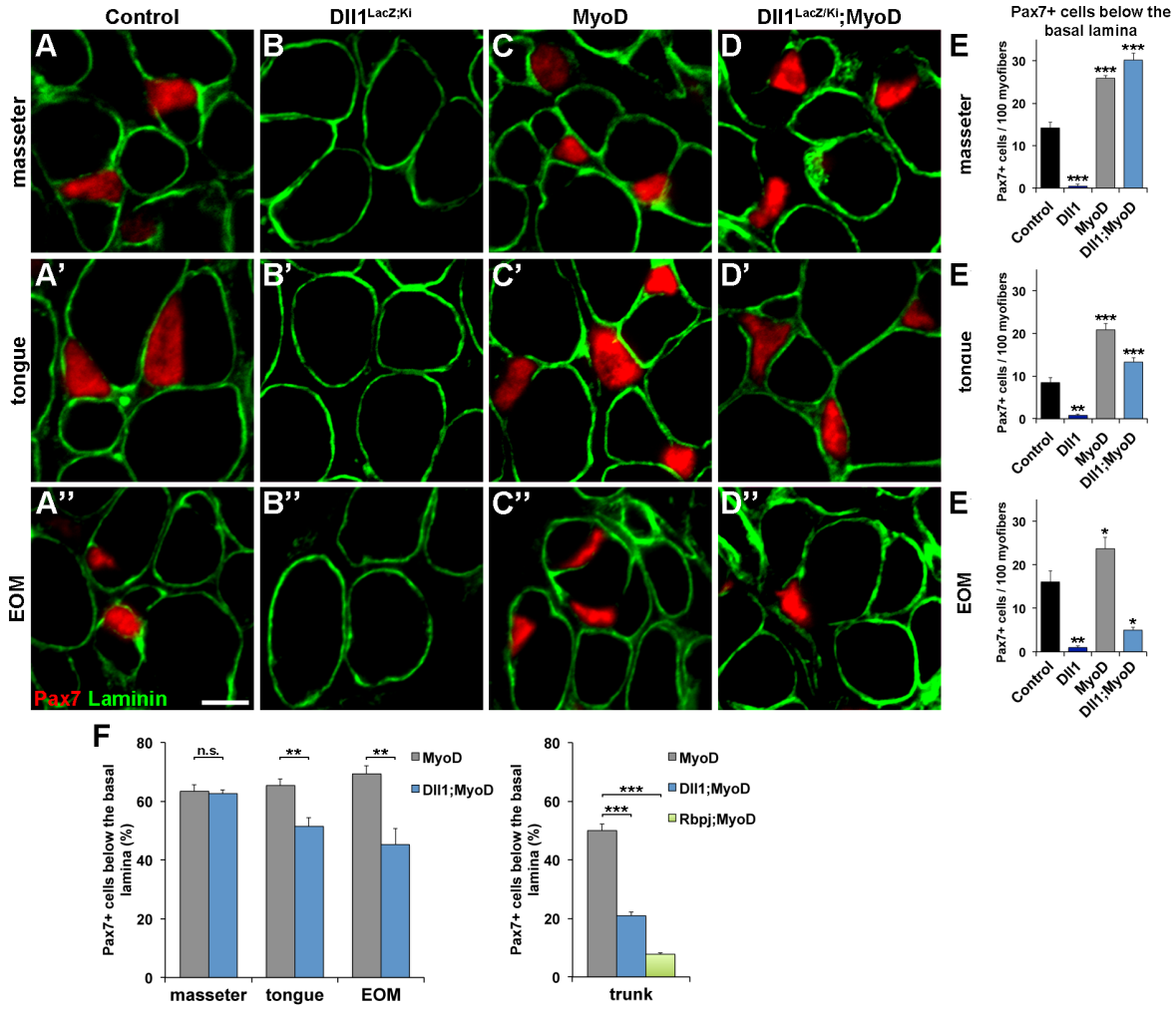

Figure 15. **Homing of craniofacial muscle progenitors does not depend on Notch signals**
(A-D) Analysis of the location of emerging satellite cells in their niche in different craniofacial muscle groups of control (A-A''), *Dll1*$^{lacZ/Ki}$ (B-B''), *MyoD*$^{-/-}$ (C-C'') and *Dll1*$^{lacZ/Ki}$*;MyoD*$^{-/-}$ (D-D'') mutant mice at E18. The analysis was performed by immunohistology using anti-laminin (green) and anti-Pax7 (red) antibodies. (E-E'') Quantification of the number of Pax7+ progenitor cells located below the basal lamina in the different craniofacial muscle groups as number of cells/100 myofibers. (F) Quantification of the percentage of all Pax7+ cells that locate below the basal lamina in craniofacial muscle is shown to the left. For comparison, the percentage of all Pax7+ cells that locate below the basal lamina in trunk muscle is shown to the right (cf. Bröhl et al., 2012). Error bars, SEM.

Statistical significance is indicated (*p < 0.05; **p < 0.01; ***p < 0.001; n.s., not significant). Scale bar: 5 µm.

3.9 Myogenic precursor cells migrate correctly to the limb buds of *Integrin-β1* and *ILK* conditional mutant mice

To analyze and compare the function of Integrin-β1 and ILK in muscle development, floxed *Integrin-β1* and *ILK* alleles were used (Graus-Porta et al., 2001; Terpstra et al., 2003). Conditional mutations were introduced using mice expressing Cre-recombinase under the control of Pax3 regulatory elements (Lang et al., 2005), resulting in recombination in somites. Mutations were thus introduced a substantial time before the first myogenic progenitor cells or muscle fibers form in the myotome.

Analysis of the migration of myogenic precursor cells into the limbs of conditional *Integrin-β1* and *ILK* mutant mice revealed normal cell distribution. At E11, Lbx1-positive progenitor cells were found in appropriate number and distribution in the limb buds of conditional mutant mice (Fig. 16A-C). In addition, differentiation, as assessed by MyoG and MyoD expression, was unchanged at E12.5 (Fig. 16D-G).

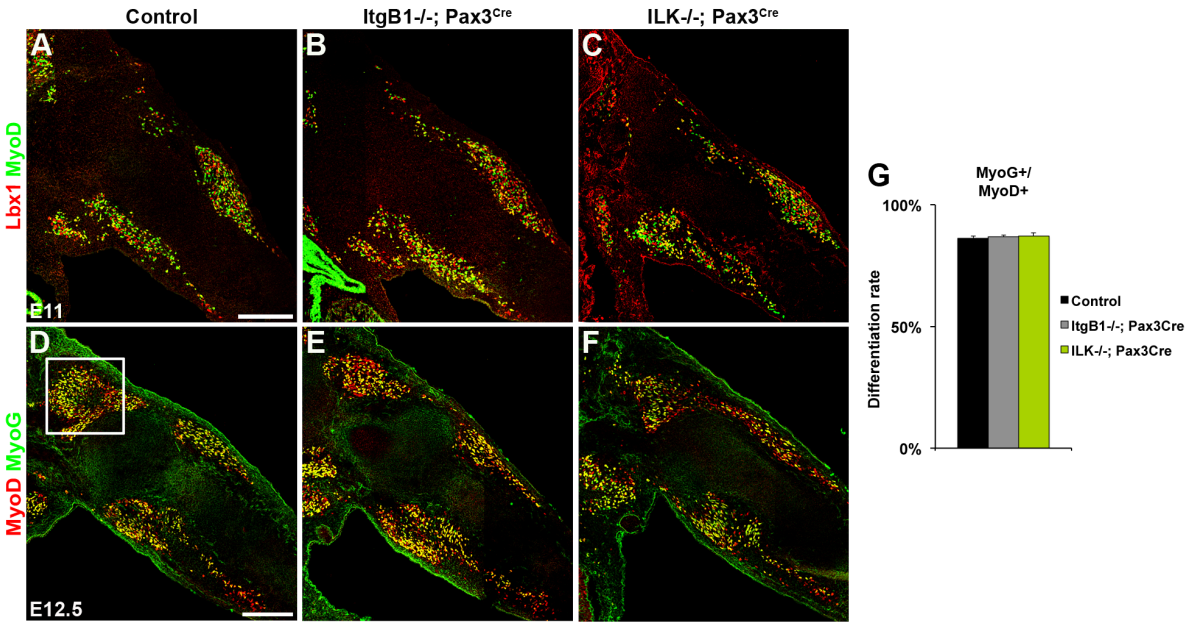

Figure 16. **Distribution of myogenic cells in the limb buds of conditional *Integrin-β1* and *ILK* mutant mice**
Immunohistological analysis of myogenic cells in the limb buds of control (A, D), conditional *Integrin-β1* (B, E), and conditional *ILK* (C, F) mutant mice at E11 (A-C) and E12.5 (D-F). Myogenic precursor cells were identified using antibodies directed against Lbx1 (red) and MyoD (green) in (A-C), and MyoG (green) and MyoD (red) in (D-F). (G) Ratio of MyoG+/MyoD+ cells in the forelimb in control and conditional *Integrin-β1* or *ILK* mutant mice at E12.5. Error bar, SEM. Scale bars: 200 µm.

3.10 Impaired myoblast fusion in conditional *Integrin-β1* and *ILK* mutant mice

In order to investigate the role of Integrin-β1 and ILK in myogenesis, sections of proximal forelimbs of E14 animals were stained using antibodies directed against MyoD and desmin. Although the groups of myogenic cells were located at the appropriate positions in conditional *Integrin-β1* and *ILK* mutant mice, the size of the groups was strongly reduced (Fig. 17A-C). In longitudinal sections, muscle fibers appeared short and disorganized, indicating that myoblast fusion was impaired (Fig. 17A'-C').

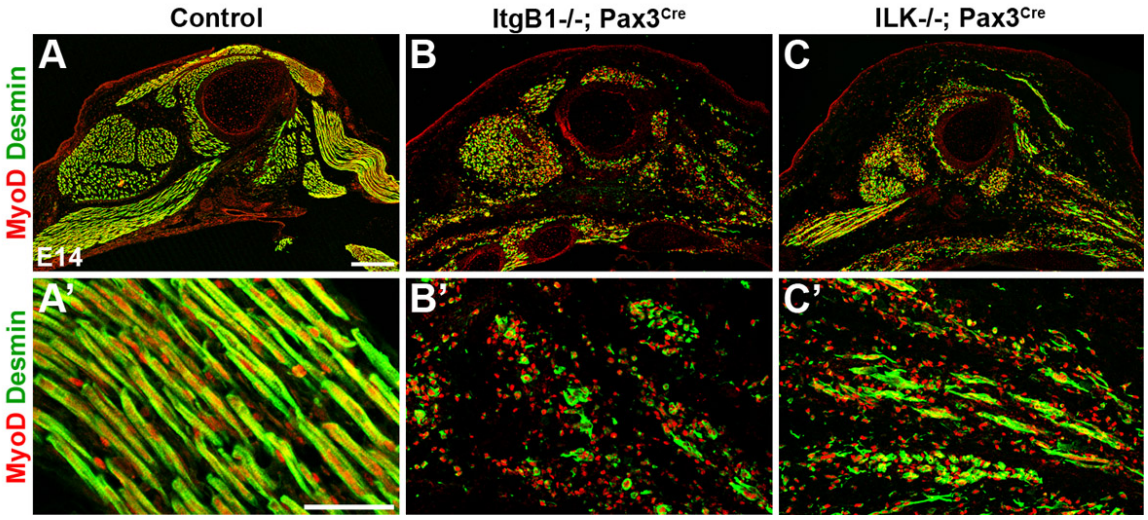

Figure 17. **Disrupted myoblast fusion in conditional *Integrin-β1* and *ILK* mutant mice**
(A-C) Immunohistological analysis of myogenic cells using antibodies directed against MyoD (red) and desmin (green) in the proximal forelimbs of control (A) and conditional *Integrin-β1* (B) and *ILK* (C) mutant animals. (A'-C') Longitudinal sections of muscle fibers of control and conditional mutant mice. Scale bars: (A-C) 300 µm, (A'-C') 50 µm.

Staining for cleaved Caspase-3 revealed increased levels of apoptosis in the muscles of conditional mutant mice, indicating that cell death contributes to the reduction in the size of the emerging muscle groups (Fig. 18A-C).

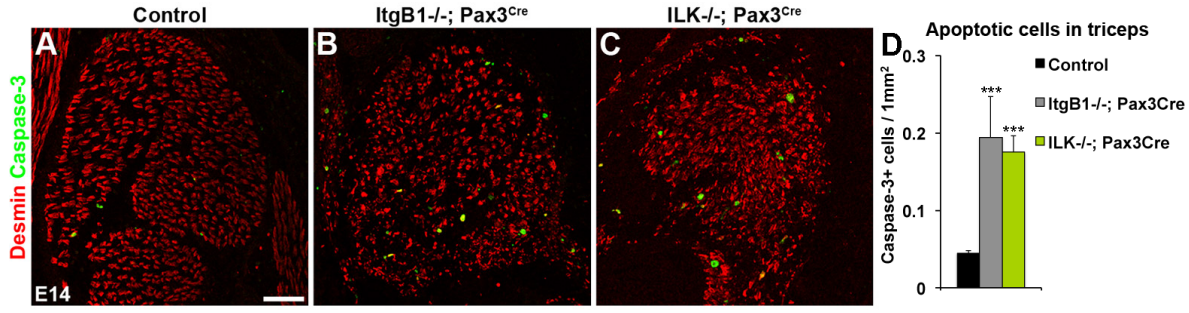

Figure 18. **Increased amount of apoptotic cells in the muscles of conditional mutant mice**

(A-C) Immunohistological analysis of proximal forelimbs of control and conditional mutant animals at E14 using antibodies directed against desmin (red) and cleaved Caspase-3 (green) marking apoptotic cells. (D) Quantification of the number of Caspase-3+ cells per 1mm^2 of triceps muscle. Error bars, SEM. Statistical significance is indicated (***p < 0.001). Scale bar: 100 µm.

3.11 Loss of muscle tissue in conditional mutant mice

To analyze the phenotype at late developmental stage, sections of the E18 proximal forelimb were stained using antibodies directed against desmin and laminin. In conditional mutant animals, the majority of muscle groups were absent. *Triceps brachii* muscle was one of the few muscle groups present in the mutant animals, however this muscle was much smaller than the one found in control mice (Fig. 19).

Figure 19. **Reduction of muscle size in conditional *Integrin-β1* and *ILK* mutant mice**
Immunohistological analysis of proximal forelimbs of control (A), conditional *Integrin-β1* (B) and conditional *ILK* (C) mutant animals at E18 using antibodies directed against desmin (green) and laminin (red). Scale bar: 500 µm.

3.12 Impaired myoblast fusion of cultured myogenic cells

To assess myoblast fusion, cells were isolated from limbs of E14 animals, plated and cultured for 72h in differentiation medium. Muscle fibers and myogenic cells were identified by the use of anti-desmin and anti-MyoD antibodies, respectively. A striking change in the ratio of multinucleated myotubes and single myoblasts

was observed in conditional *Integrin-β1* mutant mice compared to control animals. A reduction of multinucleated myofibers was also observed in conditional *ILK* mutant mice, which was however less pronounced (Fig. 20A-C). The fusion index was calculated as a ratio of the number of nuclei inside multinucleated muscle cells to the number of total myogenic nuclei. In control cultures, 75% of the MyoD+ nuclei were present in myotubes, but only 19% of the MyoD+ nuclei had fused in conditional *Integrin-β1* mutant mice. In conditional *ILK* mutant animals, MyoD+ nuclei (68%) present in myotubes were reduced (Fig. 20D). The average number of nuclei in multinucleated cells differed also. 64% of the myogenic nuclei were present in the myotubes containing 3 or more nuclei when cells from control mice were allowed to fuse. Only 6% or 47% of the nuclei in cultures of myoblasts isolated from *Integrin-β1* and *ILK* mutant animals, respectively, were located in myotubes containing 3 or more nuclei (Fig. 20E).

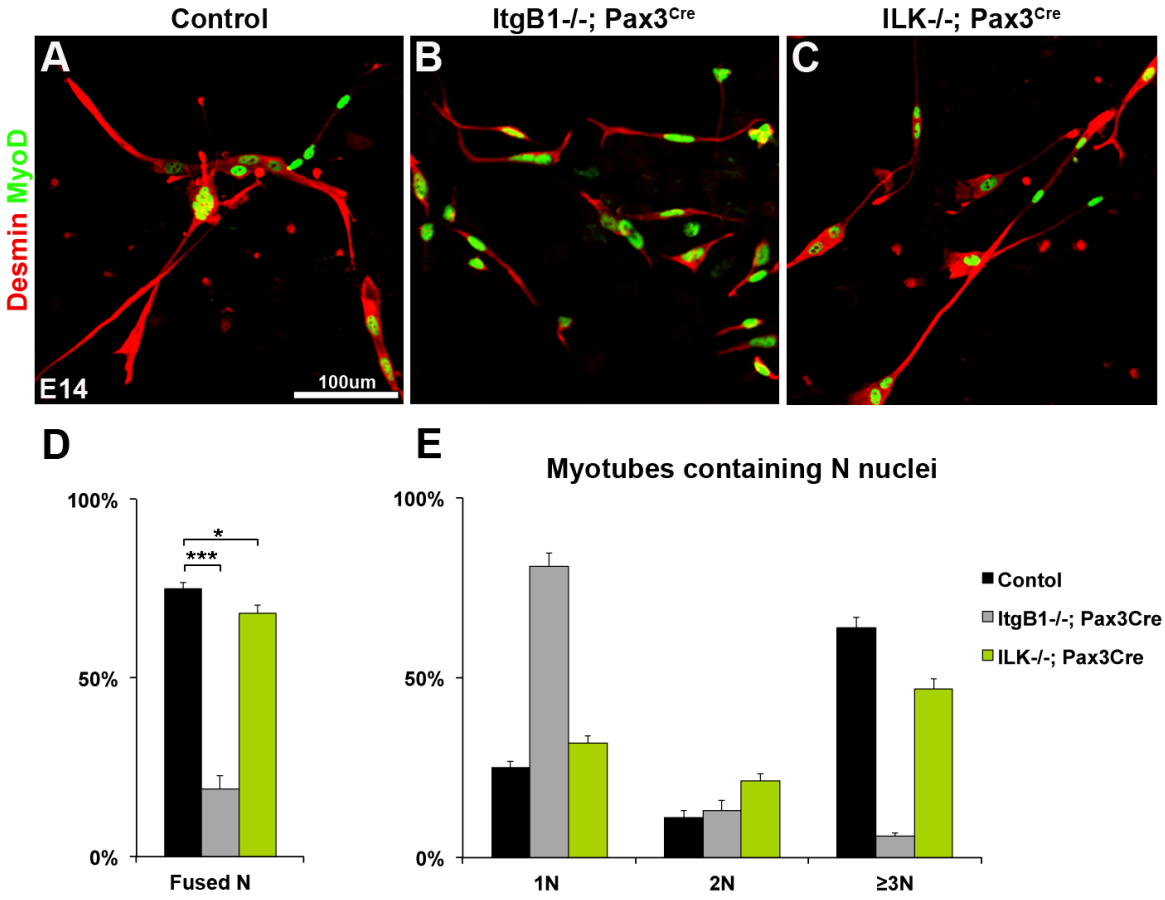

Figure 20. **Impaired myoblast fusion of cultured myogenic cells from conditional *Integrin-β1* and *ILK* mutant mice**
(A-C) Immunohistological analysis of myogenic cells isolated from the limbs of control (A), conditional *Integrin-β1* (B) and *ILK* (C) mutant mice using antibodies directed against desmin (red) and MyoD (green). (D, E) Quantification of the fusion index and percentage of the mono- and multinucleated myogenic cells. Error bars, SEM. Statistical significance is indicated (*p < 0.05; ***p < 0.001). Scale bar: 100 µm.

3.13 Reduced myotube size in conditional mutant mice

In order to analyze the size of myotubes, the forelimbs of control, conditional *Integrin-β1* and *ILK* mutant mice were dissected at E18. Myotubes dissociated during digestion procedure were plated in medium to allow their attachment to the dish, and stained using antibodies directed against desmin and MyoD. The majority of the myotubes isolated from control mice were large and contained more than 11 nuclei (Fig. 21A, E). In contrast, 95% of the myogenic cells isolated from conditional *Integrin-β1* mutant mice were mononucleated, and only few small fibers were found (Fig. 21B, E). Myotubes isolated from conditional *ILK* mutant mice were shorter than those from control mice, and 70% of the isolated myogenic cells were mononuclear (Fig. 21C, E).

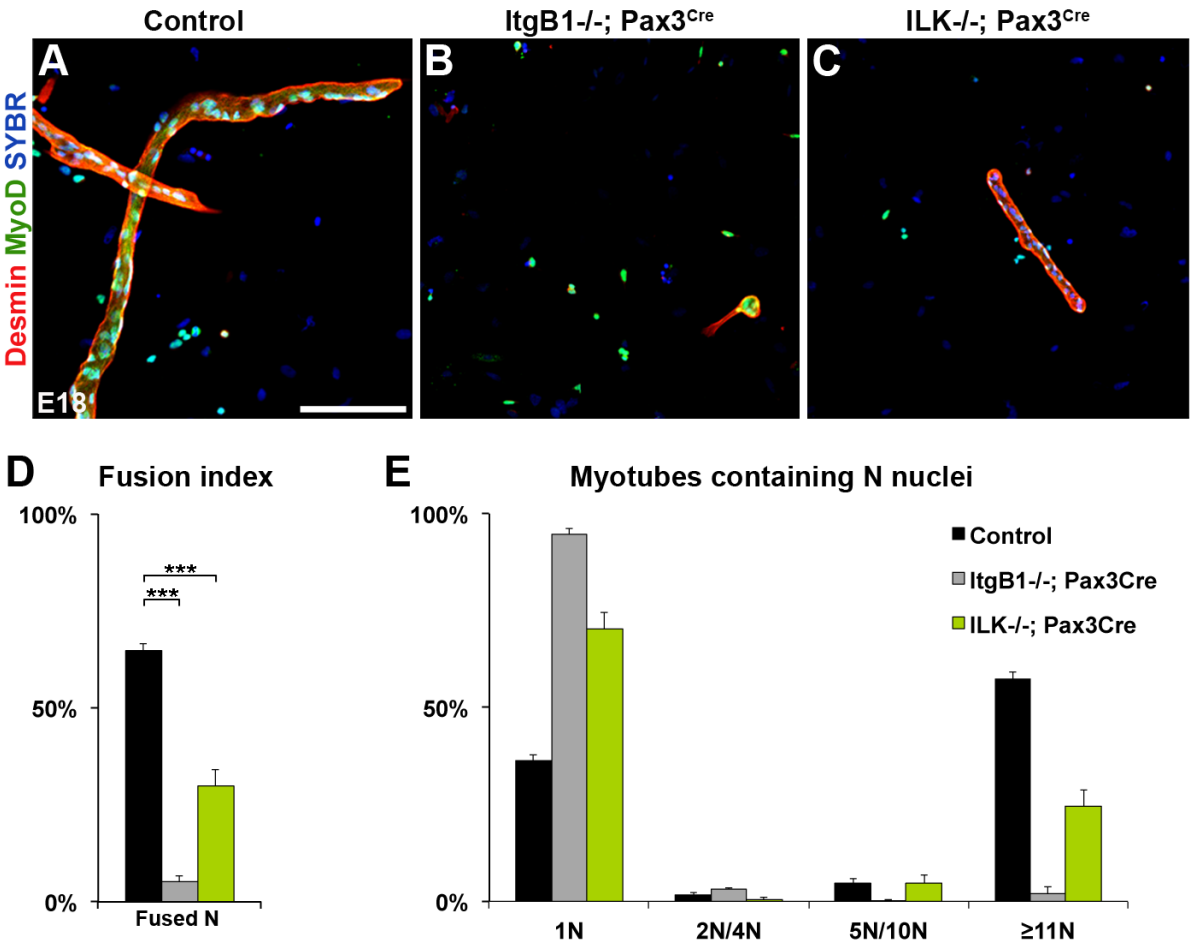

Figure 21. **Size of myotubes in conditional *Integrin-β1* and *ILK* mutant mice**
(A-C) Immunohistological analysis of myotubes isolated from the forelimbs of control (A), conditional *Integrin-β1* (B), and conditional *ILK* (C) mutant mice at E18 using antibodies directed against desmin (red) and MyoD (green). The cells were counterstained with the nuclear marker SYBR (blue). (D, E) Quantification of the fusion index and of the number of nuclei present in mono- and multinucleated cells. Error bars, SEM. Statistical significance is indicated (***p < 0.001). Scale bar: 100 µm.

3.14 Integrin-β1 is required at only one of the fusion partners

To answer the question whether Integrin-β1 is essential in both fusion partners, I mixed cells from control and *Integrin-β1* mutants. One cell type expressed yellow fluorescent protein (YFP) from the *Rosa* locus. YFP-positive control cells (from *Rosa*^{YFP};*Pax3*^{Cre} mice) fused efficiently to unlabeled control cells forming

myotubes. Similarly, *Integrin-β1* mutant YFP-positive cells fused efficiently to unlabeled control cells and formed YFP-positive myotubes (Fig. 22B). Quantification of the fusion index and of the number of mono- and multinucleated myogenic cells indicated that in the presence of control cells, conditional *Integrin-β1* mutant cells do not show fusion deficits (Fig. 22D, E). This result demonstrates that Integrin-β1 is required in one of the fusion partners.

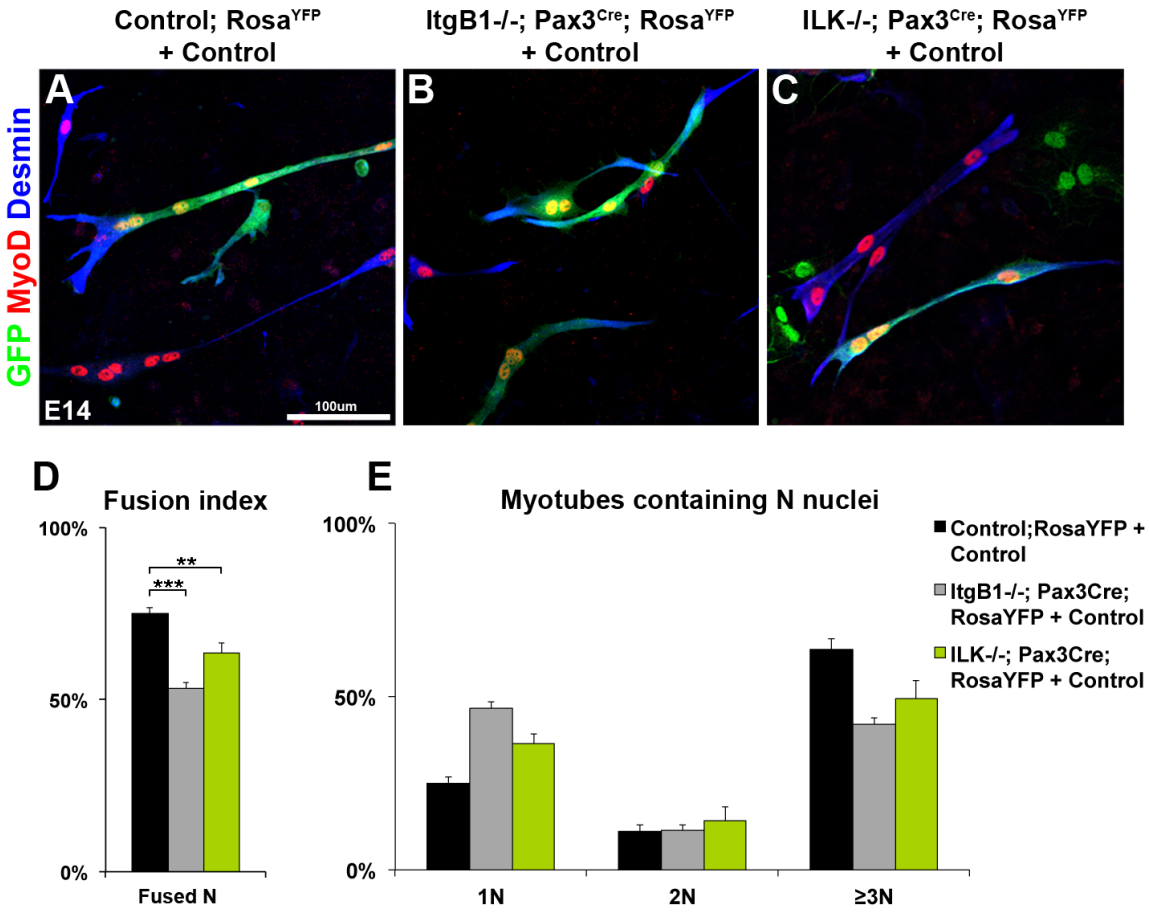

Figure 22. **Mixed cultures of control and conditional *Integrin-β1* or *ILK* mutant cells marked by the expression of YFP**
YFP-positive myogenic cells derived from control (A), conditional *Integrin-β1* (B), and conditional *ILK* (C) mutant mice. (D and E) The fusion index of YFP-positive cells and the numbers of YFP-positive nuclei present in mono- and multinucleated myogenic cells were determined. Error bars, SEM. Statistical significance is indicated (**p < 0.01; ***p < 0.001). Scale bar: 100 µm.

4 Discussion

Myofibers are the building blocks of all skeletal muscles and provide a basis for their contractile function. The overall structure and function of myofibers in cranial and trunk muscle groups are similar, and craniofacial and trunk myogenesis are controlled by the same myogenic regulatory factors – Myf5, MyoD and Mrf4. Nevertheless, cranial and trunk muscle are evolutionarily distinct and differ in the expression of isoforms of skeletal muscle-specific proteins. Moreover, the regulatory network that governs the expression of myogenic regulatory factors is different in trunk and craniofacial muscle (Rudnicki et al., 1993; Tajbakhsh et al., 1997; Kitamura et al., 1999; Kelly et al., 2004; Dong et al., 2006; Sambasivan et al., 2009). These differences might account for the fact that myopathies can differentially affect various muscle groups in the head and trunk.

Notch signaling controls the entry into the myogenic program in trunk muscle, but the function of Notch in craniofacial myogenesis has been little investigated. I show here that the progenitor cell pool in craniofacial muscle of *Dll1*$^{LacZ/Ki}$ mutant mice is depleted early and that this is largely rescued by an additional mutation of *MyoD*. Thus, the decisive role of Notch in myogenesis, the suppression of progenitor cell differentiation via regulation of *MyoD* expression, is conserved in the head and trunk. However, other Notch functions differ. In particular, homing of emerging satellite cells and *Pax7* expression depend on Notch signaling in somite- but not cranial mesoderm-derived muscle.

4.1 Origin of head muscles

Skeletal muscles in the head are necessary for swallowing, eye movement and facial expression. Craniofacial muscles are a novelty in evolution and have arisen independently of trunk muscles in chordate development. Craniofacial and trunk

muscle differ in the cell type(s) they originate from. Muscles of the trunk derive from somites that in turn are generated from the paraxial mesoderm of the trunk. Cranial paraxial and splanchnic lateral mesoderm are both derivatives of the head mesoderm and can be distinguished by their position. Cranial paraxial mesoderm gives rise to EOM, whereas both, cranial paraxial and splanchnic lateral mesoderm, contribute to branchiomeric muscles (masseter and buccinator) (Grifone and Kelly, 2007; Nathan et al., 2008; Harel et al., 2009; Tzahor, 2009). Tongue and neck muscle are of mixed origin, i.e. cells from occipital somites and cranial paraxial mesoderm contribute to their formation (Huang et al., 1999; Harel et al., 2009; Theis et al., 2010).

4.2 Entry into the myogenic program

The specification of the skeletal muscle lineage in trunk and head is dependent on Myf5, MyoD and Mrf4. Mutation of one of the myogenic regulatory factors does not result in a skeletal muscle phenotype. However, in *Myf5;Mrf4;MyoD* triple mutant mice all limb and facial muscles fail to develop, indicating that these factors play redundant roles in myogenesis (Rudnicki et al., 1993; Kassar-Duchossoy et al., 2004). Transcription of *Myf5* and *MyoD* is controlled by a number of regulatory elements. Five *Myf5* enhancers and two *MyoD* enhancers are known to regulate expression in branchial arches. Recent studies demonstrated that MyoR and capsulin act directly upstream of *Myf5* and *MyoD* and coordinate the induction of myogenic regulatory factor expression levels during mouse craniofacial development (Moncaut et al., 2012).

4.3 Notch signaling controls *MyoD* and *MyoR* expression

A strong hypomorph $Dll1^{LacZ/Ki}$ mutation was previously shown to result in premature muscle differentiation and a decrease of muscle growth, leading to the formation of tiny muscle groups in the trunk and extremities. The myogenic regulatory factors MyoD and MyoG were transiently upregulated in the myotomes

and head muscles of the mutant embryos, indicating that differentiation of head muscles groups was also affected (Schuster-Gossler et al., 2007).
I have analyzed *Dll1*$^{LacZ/Ki}$ mutant mice to define the formation of craniofacial muscle and its dependence on Notch signaling. I found that masseter and extraocular muscles are very small and lack Pax7+ progenitor cells at E13 or E18. The tongue muscle originates from both, occipital somites and head mesenchyme, and was less strongly affected than other craniofacial muscles, but was nevertheless reduced in size and lacked Pax7+ cells in *Dll1*$^{LacZ/Ki}$ mice. I conclude that Notch signals are essential to maintain muscle progenitors in craniofacial muscle, and that the loss of these progenitor cells severely impaired fetal muscle growth.

Notch signaling has been previously reported to suppress myogenic differentiation *in vivo* and *in vitro* (Kopan et al., 1994; Shawber et al., 1996; Kuroda et al., 1999; Conboy and Rando, 2002; Schuster-Gossler et al., 2007; Vasyutina et al., 2007; Bjornson et al., 2012; Mourikis et al., 2012). Several molecular mechanisms by which Notch exerts its effect have been discussed (Buas and Kadesch, 2010). Ectopic expression of the Notch intracellular domain results in a *MyoD* downregulation and interferes with myoblast differentiation. Similarly, co-culture of myoblasts with cells expressing Jagged-1 (a Notch ligand) inhibits myogenesis and downregulates *MyoG* gene expression (Kopan et al., 1994; Lindsell et al., 1995). Different studies demonstrated that Notch directly activates Hes1; the *Hes1* promoter is bound by a complex that consists of the transcription factor Rbpj and the Notch intracellular domain. Overexpression of *Hes1* can block myogenesis (Jarriault et al., 1995). However, others reported that Jagged-1-mediated Notch activation inhibited myogenic differentiation in an Rbpj- and Hes1-independent manner, and that exogenous *Hes1* expression in C2C12 cells (a myogenic cell line) did not block myogenesis. These results may suggest that two pathways mediate Notch signaling: one that is Rbpj-dependent and a second that is Rbpj-independent (Shawber et al., 1996).

In addition to MyoD-dependent pathways, other Notch-dependent mechanisms might interfere with myogenesis. Notch signaling upregulates *Hey1* expression, and the Hey1 repressor is recruited to the promoter of *MyoG* and *Mef2c*. Furthermore, constitutive *Hey1* expression did not repress MyoD, but interfered with the recruitment of MyoD to the *MyoG* and *Mef2c* promoters, and this was suggested to interfere with myogenesis (Buas et al., 2010). Finally, Notch activation robustly induces *MyoR* in cultured C2C12 myoblasts, and *MyoR* overexpression is known to block myogenic differentiation. However, siRNA-mediated downregulation of *MyoR* did not rescue myogenic differentiation after Notch activation, suggesting that MyoR might contribute but is not solely responsible for the block of myogenesis (Buas et al., 2009).

In conclusion, Notch activation in C2C12 cells results in a number of changes in gene expression. Dominique Bröhl and Ines Lahmann in our laboratory have observed in *Hes1* mutant muscle a very moderate change in *MyoD* transcripts, but a strong upregulation of MyoD protein levels. Thus, other mechanisms than transcriptional regulation might participate in the Hes1-mediated repression of MyoD protein, for instance mechanisms mediated by microRNAs.

MyoR is expressed in undifferentiated myoblasts and is downregulated upon differentiation in culture. During mouse embryogenesis, *MyoR* is expressed in the skeletal muscle lineage between E10.5 and E16.5 and is downregulated during secondary myogenesis (Lu, 1999). Mice lacking *MyoR* develop normal craniofacial muscle although the transcripts of myogenic regulatory factors are reduced in branchial arches at E9.5 (Lu, 2002; Moncaut, 2012). In *MyoR*;*capsulin* double mutant mice, mastication muscles are affected, but other muscles derived from the first arch and somites appear unchanged (Moncaut et al., 2012). However, data in C2C12 cells seem to indicate the opposite function of MyoR, since *MyoR* overexpression interferes with their myogenic differentiation. Thus, genetic data in mice and data obtained by the analysis of C2C12 cells indicate apparently different functions of MyoR.

MyoR is not expressed in extraocular muscle, but in other craniofacial and trunk muscle groups *MyoR* transcripts are observable and *MyoR* is strongly downregulated in *Dll1*$^{LacZ/Ki}$ and *Dll1*$^{LacZ/Ki}$*;MyoD*$^{-/-}$ mutants. Nevertheless, *MyoD* ablation on a *Dll1*$^{LacZ/Ki}$ mutant background does not rescue *MyoR* expression, but rescues myogenic phenotypes, indicating that downregulation of *MyoR* is not of major importance for myogenesis *in vivo*.

Tbx1 and Pitx2 are major players upstream of the myogenic determination genes in head muscle and required for normal activation of *Myf5* and *MyoD* in branchial arches (Kelly et al., 2004; Dong et al., 2006). However, in craniofacial muscles the expression of *Tbx1* and *Pitx2* does not depend on Notch signaling.

Recent genetic work from the laboratory of Carmen Birchmeier showed that elimination of Notch signals during mouse development leads to the loss of myogenic progenitor cells and formation of tiny muscle groups in the limb and trunk. However, upon additional *MyoD* mutation the number of Pax3+ myogenic progenitor cells reached the levels observed in control mice, but the colonization of the satellite cell niche was severely disrupted (Bröhl et al., 2012). I show here that ablation of *MyoD* in *Dll1*$^{LacZ/Ki}$ mutants rescued the deficits in growth of all craniofacial muscle. This indicates that suppression of *MyoD* is the major function of Notch in craniofacial as well as in trunk myogenesis.

Myogenic progenitors were present in all craniofacial muscle groups of the rescued *Dll1*$^{LacZ/Ki}$*;MyoD*$^{-/-}$ mutants, and the rescue of progenitors was complete in most craniofacial muscles. The exception that I observed was extraocular muscle, where the rescue of progenitors was incomplete. Thus, in addition to MyoD, other targets are essential readouts of Notch in progenitor maintenance in extraocular muscle.

4.4 Notch signals, *Pax7* expression and homing of emerging satellite cells

In trunk muscle, myogenic progenitor cells were rescued in *Dll1$^{LacZ/Ki}$;MyoD$^{-/-}$* mice, but these progenitors no longer expressed Pax7 and their identification relied thus on the use of other markers like Pax3 (Bröhl et al., 2012). Similarly, Notch signaling was reported to control *Pax7* expression in cultured satellite cells (Wen et al., 2012). I show here that in craniofacial muscle rescued progenitors express Pax7 in *Dll1$^{LacZ/Ki}$;MyoD$^{-/-}$* mice, indicating that Pax7 expression is Notch-independent in cranial myogenic progenitors. I conclude that Pax7 expression in progenitor cells of head and trunk muscle is differentially controlled by Notch signaling.

It is interesting to note that in *Dll1$^{LacZ/Ki}$;MyoD$^{-/-}$* double mutant mice, Pax7-positive cells are restored in the extrinsic part of the tongue derived from head mesoderm. However, the intrinsic, somite-derived tongue muscle contains very few Pax7 expressing cells. Nevertheless, in the double mutants muscle growth is rescued in both portions of the tongue. It is possible that similar to trunk muscle, rescued myogenic progenitor cells in intrinsic tongue no longer express Pax7. To verify this hypothesis, I am currently performing experiments and test for markers to identify such cells.

I show here that the impact of Notch on homing of satellite cells is different in head and trunk muscle. Satellite cells locate below the basal lamina of the muscle fiber, which starts to appear around E15.5, and emerging satellite cells are first detectable in their niche at this stage. In trunk muscle, progenitor cells fail to assume a satellite cell position, i.e. the proportion of interstitial cells is considerably larger in *Dll1$^{LacZ/Ki}$;MyoD$^{-/-}$ or Rbpj$^{-/-}$;MyoD$^{-/-}$* than in *MyoD$^{-/-}$* mutants (Bröhl et al., 2012). We assigned this to deficits in the assembly of a basal lamina around emerging satellite cells and impaired myofiber adhesion. In contrast, similar proportions of progenitor cells homed correctly in masseter and the

extrinsic part of tongue muscle of *Dll1$^{LacZ/Ki}$;MyoD$^{-/-}$ and MyoD$^{-/-}$* mutants. Satellite cells of extraocular muscle displayed a homing deficit, but this change was very subtle compared to the one observed previously in trunk muscle. I conclude that the role of Notch signaling differentially affects colonization of the niche by satellite cells generated from head and somitic mesoderm.

Remarkably, loss of Pax7 expressing myogenic progenitors and homing deficit are diverge in conditional *DnMaml;MyoD$^{-/-}$* double mutant mice. Thus, Dominique Bröhl noted that in *coDnMaml;MyoD$^{-/-}$* trunk muscle, progenitor cells expressed Pax7 but nevertheless were unable to home correctly. Therefore, loss of Pax7 cannot account for the homing deficit of satellite cells in *Dll1$^{LacZ/Ki}$;MyoD$^{-/-}$* muscle.

4.5 Mouse myoblast fusion

Muscle fibers are multinucleated syncytia that arise from the fusion of mononucleated myoblasts and play a crucial role in muscle function (Jansen, 2008). Formation of embryonic muscle fibers occurs in two phases: primary myogenesis, in which the initial myofibers are generated and secondary myogenesis, in which the primary fibers increase in size and additional fibers are formed. On a cellular level, the fusion is characterized by adhesion, alignment of myoblast membranes, followed by the formation of a specialized membrane microdomain at the contact sites and the subsequent fusion of the cells. In *Drosophila*, adhesion of myoblasts in mediated by Ig-superfamily proteins (Bour et al., 2000; Ruiz-Gomez et al., 2000; Strunkelnberg et al., 2001). At the site of fusion, F-actin-rich structures bring the membranes into close proximity, and this is a prerequisite for the formation of a fusion pore where the membrane breaks down. The fusion pore then expands and the nucleus is added to the growing myotube.

Genetic analyses indicated that a molecular cascade that controls actin polymerization, consisting of Rac GTPases, Rac regulators, WASp nucleation

promoting factor, and the Arp2/3 complex is essential for fusion in *Drosophila* (Luo et al., 1994; Richardson et al., 2007; Schafer et al., 2007). Previous studies performed in our laboratory indicated that the small G-proteins Rac1 and Cdc42 play an essential role in mouse myoblast fusion (Vasyutina 2009). Rac1 and Cdc42 can regulate actin dynamics, formation of plasma membrane protrusion, and vesicle traffic.

4.6 Integrin-β1 and ILK are essential for myoblast fusion

Integrins are receptors that mediate cell adhesion, either to the extracellular matrix or to other cells. Integrins can also provide intracellular signals and thereby define cellular shape, motility, and participate in the control of proliferation. Previous data have shown that Integrin-β1 is essential for myogenic fusion. This was analyzed using Cre recombinase under control of the human skeletal alpha-actin (HSA) promoter that introduced the conditional mutation in *Integrin-β1*. However, the myoblast fusion phenotype observed in such mice was relatively mild (Schwander et al., 2003). Integrin-linked kinase (ILK) is a multifunctional protein that binds β-integrin cytoplasmic domains and regulates actin dynamics by recruiting actin binding regulatory proteins such as alpha- and beta-parvin. Conditional *ILK* mutant mice – the mutation was introduced by an independently generated HSA^{Cre} line – developed a mild progressive muscle dystrophy mainly restricted to myotendinous junctions. *In vitro* analysis of *ILK* mutant myoblasts indicated that ILK does not play a role in myoblast fusion (Wang et al., 2008). Taking into consideration that using HSA^{Cre} recombination occurs late in myoblasts and time is needed to deplete the transcripts and the protein after recombination, the analysis might have underestimated the importance of Integrin-β1 and ILK in myogenesis. I used $Pax3^{Cre}$ to re-investigate this. $Pax3^{Cre}$ introduces mutation already in the mesoderm before somitogenesis, and thus a very substantial time before the first myogenic progenitor cells or muscle fibers form. I demonstrated that migration of myogenic precursor cells is not affected but myoblast fusion is severely impaired in these mutant strains. The

myoblast fusion deficit in *ILK* mutant mice is very pronounced *in vivo,* but less severe than the one observed for *Integrin-β1*. *In vitro*, fusion deficits were further attenuated, indicating that under two dimensional cell culture conditions, fusion is less dependent on ILK function than *in vivo*.

4.7 Correct myogenic progenitor migration and impaired myoblast fusion

Analysis of the distribution of Lbx1-positive progenitor cells indicated that cells migrated correctly to the limb buds in the conditional *Integrin-β1* and *ILK* mutant embryos. Differentiation of myogenic precursor cells was also unaffected, as assessed by the proportion of MyoG- and MyoD-positive cells. However, pronounced differences in muscle development at subsequent stages were observed. Myofibers appeared disorganized and some muscle groups were lost at E14. The phenotype was more pronounced at E18, when only one disorganized muscle (triceps) was found in the appropriate position. I also observed increased levels of apoptotic cells in the very disorganized muscle groups.

4.8 Impaired myoblast fusion and reduced myotube size in conditional mutant mice

To investigate the role of Integrin-β1 and ILK in myotube formation *in vitro*, cells were isolated from limbs of E14 animals and cultured in differentiation medium, i.e. in medium containing little serum. Under these conditions, the cultured myogenic cells differentiate and fuse. Although the amount of myogenic cells in the cultures of *Integrin-β1*- and *ILK*-deficient myoblasts was unchanged, I observed striking differences in relative proportions of myotubes and myoblasts obtained from *Integrin-β1* mutants, reflecting a deficit in myoblast fusion. In particular, I observed that multinucleated myofibers were much more frequent in

preparations from control than from conditional *Integrin-β1* mutant mice. Such a reduction was also observable in cultures obtained from *ILK* mutants, but the reduction was less pronounced.

A very severe impact of Integrin-β1 and ILK on myoblast fusion was also observed when myotubes from prenatal conditional mutant mice were isolated and the number of nuclei in the myotubes was determined. The majority of *Integrin-β1*-deficient myoblasts had remained mononucleated and only few formed myotubes. Myotubes isolated from conditional *ILK* mutant mice were shorter than those from control mice, and the majority of the isolated myogenic cells were mononuclear. These analyses demonstrate, that Integrin-β1 and ILK play important roles in myoblast fusion both *in vitro* and *in vivo*.

In *Drosophila* myogenesis, the fusion partners are non-equivalent, and two distinct cell types participate in fusion, founder and fusion-competent cells (Bate, 1990; Dohrmann et al., 1990; Ruiz-Gomez et al., 2000). Previous results indicated that both fusion partners depend on Rac1 and Cdc42 in mice (Vasyutina et al., 2009). Therefore, I analyzed whether Integrin-β1 is also required in both fusion partners. Myogenic cells isolated from control and conditional *Integrin-β1* mutant mice were mixed in culture. Fused myotubes contained nuclei from both control and *Integrin-β1*-deficient myoblasts indicating that Integrin-β1 is required in only one of the fusion partners. Therefore, Integrin-β1 mediates not only cell-matrix, but also cell-cell adhesion.

Downstream factors that mediate integrin/ILK function in skeletal muscle development are not well understood. The scaffolding protein ILK binds the cytoplasmic tail of Integrin-β1 and organizes the actin cytoskeleton by recruiting actin-binding and actin-regulatory proteins like PINCH, parvin, paxillin and kindlin (Legate et al., 2006). In migrating fibroblasts, ILK has been shown to regulate integrin-associated rearrangement of actin filaments through a phosphatidylinositol 3-kinase/Akt/Rac1 pathway (Qian et al., 2005). To answer

the question whether Integrin-β1, ILK and Rac1 act together in a signaling pathway during myoblast fusion, Claudia Rassek and I analyzed the formation of multinucleated myofibers in mice double heterozygous for *Integrin-β1* and *Rac1* (ongoing experiments). Remarkably, double heterozygous (*Integrin-β1*$^{+/-}$*;Rac1*$^{+/-}$*; Pax3*^{Cre}) but not single heterozygous mice show a mild fusion deficit. In addition, Claudia Rassek used an activated variant of *Rac1* (*Rac1DA*; cf (Srinivasan et al., 2009) and expressed it in an *Integrin-β1* and *ILK* mutant genetic background. In this epistasis experiment, fusion deficits are substantially rescued. Thus, the genetic interactions as well as rescue experiments indicate that during myoblast fusion, integrins and Rac1 act in a linear signaling cascade.

5 Summary

Craniofacial muscles are small skeletal muscles involved in mastication, swallowing, vocalization and facial expression. In contrast to trunk and limb muscles, the majority of craniofacial muscles originate from head mesoderm. Different transcriptional mechanisms control the expression of the myogenic regulatory factors and therefore entry into the differentiation program in trunk and craniofacial muscle. Notch signaling controls trunk myogenesis, but its function in craniofacial muscle development has been little investigated. I show here that the progenitor cell pool in craniofacial muscle of *Dll1*$^{LacZ/Ki}$ mutant mice is depleted early and that this is largely rescued by an additional mutation of *MyoD*. My data show that suppression of MyoD is the major function of Notch in both, craniofacial and trunk myogenesis. However, other Notch functions differ. In particular, colonization of emerging satellite cells and *Pax7* expression is differentially affected by Notch signaling in somite- and cranial mesoderm-derived muscle.

Muscle fibers are multinucleated syncytia that arise by the fusion of mononucleated myoblasts, which allows generation, growth, and repair of muscle fibers. On a cellular level, the fusion is characterized by cell adhesion, alignment of myoblast membranes and membrane fusion. Previous work had indicated that Integrin-β1 is essential for fusion. ILK is an adaptor protein that is known to bind to the intracellular domain of Integrin-β1, and is thought to transmit integrin signals to the cytoskeleton. I tested here whether ILK is essential for myoblast fusion and directly compared Integrin-β1 and ILK phenotypes. I observed pronounced deficits in myoblast fusion in *ILK* mutant mice *in vivo,* but the phenotype was less severe than the one observed for *Integrin-β1* mutants. My data show that ILK is in part an essential downstream component of Integrin-β1 signaling in myoblast fusion, and suggest that ILK transmits Integrin signals to the cytoskeleton.

Zusammenfassung

Kraniofaziale Muskeln sind kleine Skelettmuskeln des Kopfes, die für Kauen, Schlucken, Vokalisierung und Gesichtsmimik benötigt werden. Im Gegensatz zu den Muskeln des Rumpfes und der Extremitäten stammt die Mehrheit der kraniofazialen Muskeln vom Kopfmesoderm ab. Verschiedene Transkriptionsfaktoren kontrollieren die Expression der Muskelregulationsfaktoren und somit den Eintritt in das Differenzierungsprogramm in der Muskulatur des Rumpfes und Kopfes. Der Notch-Signalweg kontrolliert die Myogenese im Rumpf, aber seine Funktion in der Entwicklung der kraniofazialen Muskeln wurde bisher nur wenig Untersucht. Ich zeige hier, dass der *pool* von Vorläuferzellen in kraniofazialen Muskeln *Dll1*$^{LacZ/Ki}$-mutanter Mäuse zu einem frühen Zeitpunkt aufgebraucht ist und dass dies durch eine zusätzliche Mutation von *MyoD* größtenteils gerettet werden kann. Meine Daten zeigen, dass die Unterdrückung von MyoD Aktivität die Hauptfunktion von Notch in der Myogenese der Kopf- **und** Rumpfmuskulatur ist. Jedoch unterscheiden sich andere Funktionen von Notch. Insbesondere unterscheiden sich Satellitenzellen, die von Somiten oder dem kranialen Mesoderm abstammen, in Bezug auf die Notch-abhängige Kolonisierung der sich bildenden Satellitenzellnische und die Expression von *Pax7*.

Muskelfasern sind multinukleäre Synzytien, die aus der Fusion von mononukleären Myoblasten hervorgehen. Myoblastenfusion läuft während der Entstehung, dem Wachstum und der Reparatur von Muskelfasern ab. Charakteristisch für die Fusion ist eine Zelladhäsion zwischen Myoblasten, die anfangs zu einer parallelen Ausrichtung der Zellmembranen führt, die dann aufgelöst werden. Genetische Arbeiten haben gezeigt, dass Integrin-β1 ein wichtiges Molekül in der Myoblastenfusion bei Mäusen ist. ILK ist ein Adaptorprotein, das die intrazelluläre Domäne von Integrin-β1 bindet und das Integrin-Signale an das Zytoskelett vermittelt. Ich habe hier untersucht, ob ILK essentiell für die Fusion von Myoblasten ist und habe die Phänotypen von Integrin-β1 und ILK direkt miteinander verglichen. Ich beobachtete ausgeprägte

Defizite in der Myoblastenfusion *ILK*-mutanter Mäuse *in vivo*, die aber weniger schwer ausgeprägt waren als die Defizite in *Integrin-β1*-Mutanten. Meine Daten zeigen, dass ILK zum Teil eine essentielle nachgeschaltete Komponente des Integrin-β1-Signalweges in der Myoblastenfusion ist und deuten darauf hin, dass ILK Integrin-Signale an das Zytoskelett vermittelt.

6 Bibliography

Aoyama, H. and Asamoto, K. (1988) 'Determination of somite cells: independence of cell differentiation and morphogenesis', *Development* 104(1): 15-28.

Artavanis-Tsakonas, S., Rand, M. D. and Lake, R. J. (1999) 'Notch signaling: cell fate control and signal integration in development', *Science* 284(5415): 770-6.

Bader, B. L., Rayburn, H., Crowley, D. and Hynes, R. O. (1998) 'Extensive vasculogenesis, angiogenesis, and organogenesis precede lethality in mice lacking all alpha v integrins', *Cell* 95(4): 507-19.

Bate, M. (1990) 'The embryonic development of larval muscles in Drosophila', *Development* 110(3): 791-804.

Beckers, J., Clark, A., Wunsch, K., Hrabe De Angelis, M. and Gossler, A. (1999) 'Expression of the mouse Delta1 gene during organogenesis and fetal development', *Mechanisms of development* 84(1-2): 165-8.

Ben-Yair, R. and Kalcheim, C. (2005) 'Lineage analysis of the avian dermomyotome sheet reveals the existence of single cells with both dermal and muscle progenitor fates', *Development* 132(4): 689-701.

Bettenhausen, B., Hrabe de Angelis, M., Simon, D., Guenet, J. L. and Gossler, A. (1995) 'Transient and restricted expression during mouse embryogenesis of Dll1, a murine gene closely related to Drosophila Delta', *Development* 121(8): 2407-18.

Birnboim, H. C. and Doly, J. (1979) 'A rapid alkaline extraction procedure for screening recombinant plasmid DNA', *Nucleic acids research* 7(6): 1513-23.

Bischoff, R. and Heintz, C. (1994) 'Enhancement of skeletal muscle regeneration', *Developmental dynamics : an official publication of the American Association of Anatomists* 201(1): 41-54.

Bjornson, C. R., Cheung, T. H., Liu, L., Tripathi, P. V., Steeper, K. M. and Rando, T. A. (2012) 'Notch signaling is necessary to maintain quiescence in adult muscle stem cells', *Stem cells* 30(2): 232-42.

Boettiger, D., Enomoto-Iwamoto, M., Yoon, H. Y., Hofer, U., Menko, A. S. and Chiquet-Ehrismann, R. (1995) 'Regulation of integrin alpha 5 beta 1 affinity during myogenic differentiation', *Developmental biology* 169(1): 261-72.

Bour, B. A., Chakravarti, M., West, J. M. and Abmayr, S. M. (2000) 'Drosophila SNS, a member of the immunoglobulin superfamily that is essential for myoblast fusion', *Genes & development* 14(12): 1498-511.

Bouvard, D., Brakebusch, C., Gustafsson, E., Aszodi, A., Bengtsson, T., Berna, A. and Fassler, R. (2001) 'Functional consequences of integrin gene mutations in mice', *Circulation research* 89(3): 211-23.

Brakebusch, C., Bouvard, D., Stanchi, F., Sakai, T. and Fassler, R. (2002) 'Integrins in invasive growth', *The Journal of clinical investigation* 109(8): 999-1006.

Braun, A., Bordoy, R., Stanchi, F., Moser, M., Kostka, G. G., Ehler, E., Brandau, O. and Fassler, R. (2003) 'PINCH2 is a new five LIM domain protein,

homologous to PINCHand localized to focal adhesions', *Experimental cell research* 284(2): 239-50.
Brennan, K. J. and Hardeman, E. C. (1993) 'Quantitative analysis of the human alpha-skeletal actin gene in transgenic mice', *The Journal of biological chemistry* 268(1): 719-25.
Bröhl, D., Vasyutina, E., Czajkowski, M. T., Griger, J., Rassek, C., Rahn, H. P., Purfurst, B., Wende, H. and Birchmeier, C. (2012) 'Colonization of the satellite cell niche by skeletal muscle progenitor cells depends on Notch signals', *Developmental cell* 23(3): 469-81.
Bronner-Fraser, M., Artinger, M., Muschler, J. and Horwitz, A. F. (1992) 'Developmentally regulated expression of alpha 6 integrin in avian embryos', *Development* 115(1): 197-211.
Buas, M. F., Kabak, S. and Kadesch, T. (2009) 'Inhibition of myogenesis by Notch: evidence for multiple pathways', *Journal of cellular physiology* 218(1): 84-93.
Buas, M. F., Kabak, S. and Kadesch, T. (2010) 'The Notch effector Hey1 associates with myogenic target genes to repress myogenesis', *The Journal of biological chemistry* 285(2): 1249-58.
Buas, M. F. and Kadesch, T. (2010) 'Regulation of skeletal myogenesis by Notch', *Experimental cell research* 316(18): 3028-33.
Buckingham, M. (2006) 'Myogenic progenitor cells and skeletal myogenesis in vertebrates', *Current opinion in genetics & development* 16(5): 525-32.
Christ, B., Brand-Saberi, B., Grim, M. and Wilting, J. (1992) 'Local signalling in dermomyotomal cell type specification', *Anatomy and embryology* 186(5): 505-10.
Christ, B. and Ordahl, C. P. (1995) 'Early stages of chick somite development', *Anatomy and embryology* 191(5): 381-96.
Collins, C. A., Olsen, I., Zammit, P. S., Heslop, L., Petrie, A., Partridge, T. A. and Morgan, J. E. (2005) 'Stem cell function, self-renewal, and behavioral heterogeneity of cells from the adult muscle satellite cell niche', *Cell* 122(2): 289-301.
Collins, C. A., Zammit, P. S., Ruiz, A. P., Morgan, J. E. and Partridge, T. A. (2007) 'A population of myogenic stem cells that survives skeletal muscle aging', *Stem cells* 25(4): 885-94.
Conboy, I. M. and Rando, T. A. (2002) 'The regulation of Notch signaling controls satellite cell activation and cell fate determination in postnatal myogenesis', *Developmental cell* 3(3): 397-409.
Couly, G. F., Coltey, P. M. and Le Douarin, N. M. (1992) 'The developmental fate of the cephalic mesoderm in quail-chick chimeras', *Development* 114(1): 1-15.
Delfini, M. C., Hirsinger, E., Pourquie, O. and Duprez, D. (2000) 'Delta 1-activated notch inhibits muscle differentiation without affecting Myf5 and Pax3 expression in chick limb myogenesis', *Development* 127(23): 5213-24.
Dohrmann, C., Azpiazu, N. and Frasch, M. (1990) 'A new Drosophila homeo box gene is expressed in mesodermal precursor cells of distinct muscles during embryogenesis', *Genes & development* 4(12A): 2098-111.

Dong, F., Sun, X., Liu, W., Ai, D., Klysik, E., Lu, M. F., Hadley, J., Antoni, L., Chen, L., Baldini, A. et al. (2006) 'Pitx2 promotes development of splanchnic mesoderm-derived branchiomeric muscle', *Development* 133(24): 4891-9.
Duxson, M. J., Usson, Y. and Harris, A. J. (1989) 'The origin of secondary myotubes in mammalian skeletal muscles: ultrastructural studies', *Development* 107(4): 743-50.
Engleka, K. A., Gitler, A. D., Zhang, M., Zhou, D. D., High, F. A. and Epstein, J. A. (2005) 'Insertion of Cre into the Pax3 locus creates a new allele of Splotch and identifies unexpected Pax3 derivatives', *Developmental biology* 280(2): 396-406.
Fassler, R. and Meyer, M. (1995) 'Consequences of lack of beta 1 integrin gene expression in mice', *Genes & development* 9(15): 1896-908.
Gardner, H., Kreidberg, J., Koteliansky, V. and Jaenisch, R. (1996) 'Deletion of integrin alpha 1 by homologous recombination permits normal murine development but gives rise to a specific deficit in cell adhesion', *Developmental biology* 175(2): 301-13.
Geiger, B., Bershadsky, A., Pankov, R. and Yamada, K. M. (2001) 'Transmembrane crosstalk between the extracellular matrix--cytoskeleton crosstalk', *Nature reviews. Molecular cell biology* 2(11): 793-805.
Georges-Labouesse, E., Messaddeq, N., Yehia, G., Cadalbert, L., Dierich, A. and Le Meur, M. (1996) 'Absence of integrin alpha 6 leads to epidermolysis bullosa and neonatal death in mice', *Nature genetics* 13(3): 370-3.
Grashoff, C., Aszodi, A., Sakai, T., Hunziker, E. B. and Fassler, R. (2003) 'Integrin-linked kinase regulates chondrocyte shape and proliferation', *EMBO reports* 4(4): 432-8.
Graus-Porta, D., Blaess, S., Senften, M., Littlewood-Evans, A., Damsky, C., Huang, Z., Orban, P., Klein, R., Schittny, J. C. and Muller, U. (2001) 'Beta1-class integrins regulate the development of laminae and folia in the cerebral and cerebellar cortex', *Neuron* 31(3): 367-79.
Grifone, R. and Kelly, R. G. (2007) 'Heartening news for head muscle development', *Trends in genetics : TIG* 23(8): 365-9.
Gros, J., Manceau, M., Thome, V. and Marcelle, C. (2005) 'A common somitic origin for embryonic muscle progenitors and satellite cells', *Nature* 435(7044): 954-8.
Hannigan, G., Troussard, A. A. and Dedhar, S. (2005) 'Integrin-linked kinase: a cancer therapeutic target unique among its ILK', *Nature reviews. Cancer* 5(1): 51-63.
Harel, I., Nathan, E., Tirosh-Finkel, L., Zigdon, H., Guimaraes-Camboa, N., Evans, S. M. and Tzahor, E. (2009) 'Distinct origins and genetic programs of head muscle satellite cells', *Developmental cell* 16(6): 822-32.
Hirsch, E., Lohikangas, L., Gullberg, D., Johansson, S. and Fassler, R. (1998) 'Mouse myoblasts can fuse and form a normal sarcomere in the absence of beta1 integrin expression', *Journal of cell science* 111 (Pt 16): 2397-409.
Hirsinger, E., Malapert, P., Dubrulle, J., Delfini, M. C., Duprez, D., Henrique, D., Ish-Horowicz, D. and Pourquie, O. (2001) 'Notch signalling acts in

postmitotic avian myogenic cells to control MyoD activation', *Development* 128(1): 107-16.
Horsley, V. and Pavlath, G. K. (2004) 'Forming a multinucleated cell: molecules that regulate myoblast fusion', *Cells, tissues, organs* 176(1-3): 67-78.
Hrabe de Angelis, M., McIntyre, J., 2nd and Gossler, A. (1997) 'Maintenance of somite borders in mice requires the Delta homologue DII1', *Nature* 386(6626): 717-21.
Huang, R., Zhi, Q., Izpisua-Belmonte, J. C., Christ, B. and Patel, K. (1999) 'Origin and development of the avian tongue muscles', *Anatomy and embryology* 200(2): 137-52.
Hynes, R. O. (2002) 'Integrins: bidirectional, allosteric signaling machines', *Cell* 110(6): 673-87.
Jarriault, S., Brou, C., Logeat, F., Schroeter, E. H., Kopan, R. and Israel, A. (1995) 'Signalling downstream of activated mammalian Notch', *Nature* 377(6547): 355-8.
Kassar-Duchossoy, L., Gayraud-Morel, B., Gomes, D., Rocancourt, D., Buckingham, M., Shinin, V. and Tajbakhsh, S. (2004) 'Mrf4 determines skeletal muscle identity in Myf5:Myod double-mutant mice', *Nature* 431(7007): 466-71.
Kassar-Duchossoy, L., Giacone, E., Gayraud-Morel, B., Jory, A., Gomes, D. and Tajbakhsh, S. (2005) 'Pax3/Pax7 mark a novel population of primitive myogenic cells during development', *Genes & development* 19(12): 1426-31.
Kelly, R. G., Jerome-Majewska, L. A. and Papaioannou, V. E. (2004) 'The del22q11.2 candidate gene Tbx1 regulates branchiomeric myogenesis', *Human molecular genetics* 13(22): 2829-40.
Kimble, J. and Simpson, P. (1997) 'The LIN-12/Notch signaling pathway and its regulation', *Annual review of cell and developmental biology* 13: 333-61.
Kitamura, K., Miura, H., Miyagawa-Tomita, S., Yanazawa, M., Katoh-Fukui, Y., Suzuki, R., Ohuchi, H., Suehiro, A., Motegi, Y., Nakahara, Y. et al. (1999) 'Mouse Pitx2 deficiency leads to anomalies of the ventral body wall, heart, extra- and periocular mesoderm and right pulmonary isomerism', *Development* 126(24): 5749-58.
Kopan, R., Nye, J. S. and Weintraub, H. (1994) 'The intracellular domain of mouse Notch: a constitutively activated repressor of myogenesis directed at the basic helix-loop-helix region of MyoD', *Development* 120(9): 2385-96.
Kreidberg, J. A., Donovan, M. J., Goldstein, S. L., Rennke, H., Shepherd, K., Jones, R. C. and Jaenisch, R. (1996) 'Alpha 3 beta 1 integrin has a crucial role in kidney and lung organogenesis', *Development* 122(11): 3537-47.
Kuroda, K., Tani, S., Tamura, K., Minoguchi, S., Kurooka, H. and Honjo, T. (1999) 'Delta-induced Notch signaling mediated by RBP-J inhibits MyoD expression and myogenesis', *The Journal of biological chemistry* 274(11): 7238-44.
Lang, D., Lu, M. M., Huang, L., Engleka, K. A., Zhang, M., Chu, E. Y., Lipner, S., Skoultchi, A., Millar, S. E. and Epstein, J. A. (2005) 'Pax3 functions at a nodal point in melanocyte stem cell differentiation', *Nature* 433(7028): 884-7.

Legate, K. R. and Fassler, R. (2009) 'Mechanisms that regulate adaptor binding to beta-integrin cytoplasmic tails', *Journal of cell science* 122(Pt 2): 187-98.
Legate, K. R., Montanez, E., Kudlacek, O. and Fassler, R. (2006) 'ILK, PINCH and parvin: the tIPP of integrin signalling', *Nature reviews. Molecular cell biology* 7(1): 20-31.
Lewis, J. (1998) 'Notch signalling and the control of cell fate choices in vertebrates', *Seminars in cell & developmental biology* 9(6): 583-9.
Lindsell, C. E., Shawber, C. J., Boulter, J. and Weinmaster, G. (1995) 'Jagged: a mammalian ligand that activates Notch1', *Cell* 80(6): 909-17.
Lu, J. R., Bassel-Duby, R., Hawkins, A., Chang, P., Valdez, R., Wu, H., Gan, L., Shelton, J. M., Richardson, J. A. and Olson, E. N. (2002) 'Control of facial muscle development by MyoR and capsulin', *Science* 298(5602): 2378-81.
Luo, B. H. and Springer, T. A. (2006) 'Integrin structures and conformational signaling', *Current opinion in cell biology* 18(5): 579-86.
Luo, L., Liao, Y. J., Jan, L. Y. and Jan, Y. N. (1994) 'Distinct morphogenetic functions of similar small GTPases: Drosophila Drac1 is involved in axonal outgrowth and myoblast fusion', *Genes & development* 8(15): 1787-802.
Mauro, A. (1961) 'Satellite cell of skeletal muscle fibers', *The Journal of biophysical and biochemical cytology* 9: 493-5.
Mayer, U., Saher, G., Fassler, R., Bornemann, A., Echtermeyer, F., von der Mark, H., Miosge, N., Poschl, E. and von der Mark, K. (1997) 'Absence of integrin alpha 7 causes a novel form of muscular dystrophy', *Nature genetics* 17(3): 318-23.
McDonald, K. A., Lakonishok, M. and Horwitz, A. F. (1995) 'Alpha v and alpha 3 integrin subunits are associated with myofibrils during myofibrillogenesis', *Journal of cell science* 108 (Pt 3): 975-83.
McMahon, J. A., Takada, S., Zimmerman, L. B., Fan, C. M., Harland, R. M. and McMahon, A. P. (1998) 'Noggin-mediated antagonism of BMP signaling is required for growth and patterning of the neural tube and somite', *Genes & development* 12(10): 1438-52.
Moncaut, N., Cross, J. W., Siligan, C., Keith, A., Taylor, K., Rigby, P. W. and Carvajal, J. J. (2012) 'Musculin and TCF21 coordinate the maintenance of myogenic regulatory factor expression levels during mouse craniofacial development', *Development* 139(5): 958-67.
Mourikis, P., Sambasivan, R., Castel, D., Rocheteau, P., Bizzarro, V. and Tajbakhsh, S. (2012) 'A critical requirement for notch signaling in maintenance of the quiescent skeletal muscle stem cell state', *Stem cells* 30(2): 243-52.
Nathan, E., Monovich, A., Tirosh-Finkel, L., Harrelson, Z., Rousso, T., Rinon, A., Harel, I., Evans, S. M. and Tzahor, E. (2008) 'The contribution of Islet1-expressing splanchnic mesoderm cells to distinct branchiomeric muscles reveals significant heterogeneity in head muscle development', *Development* 135(4): 647-57.
Nikolopoulos, S. N. and Turner, C. E. (2000) 'Actopaxin, a new focal adhesion protein that binds paxillin LD motifs and actin and regulates cell adhesion', *The Journal of cell biology* 151(7): 1435-48.

Noden, D. M. (1983) 'The embryonic origins of avian cephalic and cervical muscles and associated connective tissues', *The American journal of anatomy* 168(3): 257-76.
Noden, D. M. and Trainor, P. A. (2005) 'Relations and interactions between cranial mesoderm and neural crest populations', *Journal of anatomy* 207(5): 575-601.
Olski, T. M., Noegel, A. A. and Korenbaum, E. (2001) 'Parvin, a 42 kDa focal adhesion protein, related to the alpha-actinin superfamily', *Journal of cell science* 114(Pt 3): 525-38.
Ono, Y., Boldrin, L., Knopp, P., Morgan, J. E. and Zammit, P. S. (2010) 'Muscle satellite cells are a functionally heterogeneous population in both somite-derived and branchiomeric muscles', *Developmental biology* 337(1): 29-41.
Ontell, M. and Kozeka, K. (1984) 'Organogenesis of the mouse extensor digitorum logus muscle: a quantitative study', *The American journal of anatomy* 171(2): 149-61.
Ordahl, C. P. (1992) 'Developmental regulation of sarcomeric gene expression', *Current topics in developmental biology* 26: 145-68.
Potocnik, A. J., Brakebusch, C. and Fassler, R. (2000) 'Fetal and adult hematopoietic stem cells require beta1 integrin function for colonizing fetal liver, spleen, and bone marrow', *Immunity* 12(6): 653-63.
Qian, Y., Zhong, X., Flynn, D. C., Zheng, J. Z., Qiao, M., Wu, C., Dedhar, S., Shi, X. and Jiang, B. H. (2005) 'ILK mediates actin filament rearrangements and cell migration and invasion through PI3K/Akt/Rac1 signaling', *Oncogene* 24(19): 3154-65.
Relaix, F., Demignon, J., Laclef, C., Pujol, J., Santolini, M., Niro, C., Lagha, M., Rocancourt, D., Buckingham, M. and Maire, P. (2013) 'Six homeoproteins directly activate Myod expression in the gene regulatory networks that control early myogenesis', *PLoS genetics* 9(4): e1003425.
Relaix, F., Rocancourt, D., Mansouri, A. and Buckingham, M. (2005) 'A Pax3/Pax7-dependent population of skeletal muscle progenitor cells', *Nature* 435(7044): 948-53.
Reshef, R., Maroto, M. and Lassar, A. B. (1998) 'Regulation of dorsal somitic cell fates: BMPs and Noggin control the timing and pattern of myogenic regulator expression', *Genes & development* 12(3): 290-303.
Richardson, B. E., Beckett, K., Nowak, S. J. and Baylies, M. K. (2007) 'SCAR/WAVE and Arp2/3 are crucial for cytoskeletal remodeling at the site of myoblast fusion', *Development* 134(24): 4357-67.
Rosen, G. D., Sanes, J. R., LaChance, R., Cunningham, J. M., Roman, J. and Dean, D. C. (1992) 'Roles for the integrin VLA-4 and its counter receptor VCAM-1 in myogenesis', *Cell* 69(7): 1107-19.
Rudnicki, M. A., Braun, T., Hinuma, S. and Jaenisch, R. (1992) 'Inactivation of MyoD in mice leads to up-regulation of the myogenic HLH gene Myf-5 and results in apparently normal muscle development', *Cell* 71(3): 383-90.
Rudnicki, M. A., Schnegelsberg, P. N., Stead, R. H., Braun, T., Arnold, H. H. and Jaenisch, R. (1993) 'MyoD or Myf-5 is required for the formation of skeletal muscle', *Cell* 75(7): 1351-9.

Ruiz-Gomez, M., Coutts, N., Price, A., Taylor, M. V. and Bate, M. (2000) 'Drosophila dumbfounded: a myoblast attractant essential for fusion', *Cell* 102(2): 189-98.

Saiki, R. K., Scharf, S., Faloona, F., Mullis, K. B., Horn, G. T., Erlich, H. A. and Arnheim, N. (1985) 'Enzymatic amplification of beta-globin genomic sequences and restriction site analysis for diagnosis of sickle cell anemia', *Science* 230(4732): 1350-4.

Sakai, T., Li, S., Docheva, D., Grashoff, C., Sakai, K., Kostka, G., Braun, A., Pfeifer, A., Yurchenco, P. D. and Fassler, R. (2003) 'Integrin-linked kinase (ILK) is required for polarizing the epiblast, cell adhesion, and controlling actin accumulation', *Genes & development* 17(7): 926-40.

Sambasivan, R., Gayraud-Morel, B., Dumas, G., Cimper, C., Paisant, S., Kelly, R. G. and Tajbakhsh, S. (2009) 'Distinct regulatory cascades govern extraocular and pharyngeal arch muscle progenitor cell fates', *Developmental cell* 16(6): 810-21.

Sastry, S. K., Lakonishok, M., Thomas, D. A., Muschler, J. and Horwitz, A. F. (1996) 'Integrin alpha subunit ratios, cytoplasmic domains, and growth factor synergy regulate muscle proliferation and differentiation', *The Journal of cell biology* 133(1): 169-84.

Schafer, G., Weber, S., Holz, A., Bogdan, S., Schumacher, S., Muller, A., Renkawitz-Pohl, R. and Onel, S. F. (2007) 'The Wiskott-Aldrich syndrome protein (WASP) is essential for myoblast fusion in Drosophila', *Developmental biology* 304(2): 664-74.

Schuster-Gossler, K., Cordes, R. and Gossler, A. (2007) 'Premature myogenic differentiation and depletion of progenitor cells cause severe muscle hypotrophy in Delta1 mutants', *Proceedings of the National Academy of Sciences of the United States of America* 104(2): 537-42.

Schwander, M., Leu, M., Stumm, M., Dorchies, O. M., Ruegg, U. T., Schittny, J. and Muller, U. (2003) 'Beta1 integrins regulate myoblast fusion and sarcomere assembly', *Developmental cell* 4(5): 673-85.

Shawber, C., Nofziger, D., Hsieh, J. J., Lindsell, C., Bogler, O., Hayward, D. and Weinmaster, G. (1996) 'Notch signaling inhibits muscle cell differentiation through a CBF1-independent pathway', *Development* 122(12): 3765-73.

Sohn, R. L., Huang, P., Kawahara, G., Mitchell, M., Guyon, J., Kalluri, R., Kunkel, L. M. and Gussoni, E. (2009) 'A role for nephrin, a renal protein, in vertebrate skeletal muscle cell fusion', *Proceedings of the National Academy of Sciences of the United States of America* 106(23): 9274-9.

Song, W. K., Wang, W., Sato, H., Bielser, D. A. and Kaufman, S. J. (1993) 'Expression of alpha 7 integrin cytoplasmic domains during skeletal muscle development: alternate forms, conformational change, and homologies with serine/threonine kinases and tyrosine phosphatases', *Journal of cell science* 106 (Pt 4): 1139-52.

Srinivas, S., Watanabe, T., Lin, C. S., William, C. M., Tanabe, Y., Jessell, T. M. and Costantini, F. (2001) 'Cre reporter strains produced by targeted insertion of EYFP and ECFP into the ROSA26 locus', *BMC developmental biology* 1: 4.

Srinivasan, L., Sasaki, Y., Calado, D. P., Zhang, B., Paik, J. H., DePinho, R. A., Kutok, J. L., Kearney, J. F., Otipoby, K. L. and Rajewsky, K. (2009) 'PI3 kinase signals BCR-dependent mature B cell survival', *Cell* 139(3): 573-86.

Strunkelnberg, M., Bonengel, B., Moda, L. M., Hertenstein, A., de Couet, H. G., Ramos, R. G. and Fischbach, K. F. (2001) 'rst and its paralogue kirre act redundantly during embryonic muscle development in Drosophila', *Development* 128(21): 4229-39.

Tajbakhsh, S., Rocancourt, D., Cossu, G. and Buckingham, M. (1997) 'Redefining the genetic hierarchies controlling skeletal myogenesis: Pax-3 and Myf-5 act upstream of MyoD', *Cell* 89(1): 127-38.

Taverna, D., Disatnik, M. H., Rayburn, H., Bronson, R. T., Yang, J., Rando, T. A. and Hynes, R. O. (1998) 'Dystrophic muscle in mice chimeric for expression of alpha5 integrin', *The Journal of cell biology* 143(3): 849-59.

Terpstra, L., Prud'homme, J., Arabian, A., Takeda, S., Karsenty, G., Dedhar, S. and St-Arnaud, R. (2003) 'Reduced chondrocyte proliferation and chondrodysplasia in mice lacking the integrin-linked kinase in chondrocytes', *The Journal of cell biology* 162(1): 139-48.

Theis, S., Patel, K., Valasek, P., Otto, A., Pu, Q., Harel, I., Tzahor, E., Tajbakhsh, S., Christ, B. and Huang, R. (2010) 'The occipital lateral plate mesoderm is a novel source for vertebrate neck musculature', *Development* 137(17): 2961-71.

Tu, Y., Huang, Y., Zhang, Y., Hua, Y. and Wu, C. (2001) 'A new focal adhesion protein that interacts with integrin-linked kinase and regulates cell adhesion and spreading', *The Journal of cell biology* 153(3): 585-98.

Tu, Y., Li, F. and Wu, C. (1998) 'Nck-2, a novel Src homology2/3-containing adaptor protein that interacts with the LIM-only protein PINCH and components of growth factor receptor kinase-signaling pathways', *Molecular biology of the cell* 9(12): 3367-82.

Tzahor, E. (2009) 'Heart and craniofacial muscle development: a new developmental theme of distinct myogenic fields', *Developmental biology* 327(2): 273-9.

Tzahor, E. and Evans, S. M. (2011) 'Pharyngeal mesoderm development during embryogenesis: implications for both heart and head myogenesis', *Cardiovascular research* 91(2): 196-202.

Vasyutina, E., Lenhard, D. C., Wende, H., Erdmann, B., Epstein, J. A. and Birchmeier, C. (2007) 'RBP-J (Rbpsuh) is essential to maintain muscle progenitor cells and to generate satellite cells', *Proceedings of the National Academy of Sciences of the United States of America* 104(11): 4443-8.

Vasyutina, E., Martarelli, B., Brakebusch, C., Wende, H. and Birchmeier, C. (2009) 'The small G-proteins Rac1 and Cdc42 are essential for myoblast fusion in the mouse', *Proceedings of the National Academy of Sciences of the United States of America* 106(22): 8935-40.

von Scheven, G., Bothe, I., Ahmed, M. U., Alvares, L. E. and Dietrich, S. (2006) 'Protein and genomic organisation of vertebrate MyoR and Capsulin genes and their expression during avian development', *Gene expression patterns : GEP* 6(4): 383-93.

Wang, H. V., Chang, L. W., Brixius, K., Wickstrom, S. A., Montanez, E., Thievessen, I., Schwander, M., Muller, U., Bloch, W., Mayer, U. et al. (2008) 'Integrin-linked kinase stabilizes myotendinous junctions and protects muscle from stress-induced damage', *The Journal of cell biology* 180(5): 1037-49.

Wen, Y., Bi, P., Liu, W., Asakura, A., Keller, C. and Kuang, S. (2012) 'Constitutive Notch activation upregulates Pax7 and promotes the self-renewal of skeletal muscle satellite cells', *Molecular and cellular biology* 32(12): 2300-11.

Wu, C. (2005) 'PINCH, N(i)ck and the ILK: network wiring at cell-matrix adhesions', *Trends in cell biology* 15(9): 460-6.

Yamaji, S., Suzuki, A., Sugiyama, Y., Koide, Y., Yoshida, M., Kanamori, H., Mohri, H., Ohno, S. and Ishigatsubo, Y. (2001) 'A novel integrin-linked kinase-binding protein, affixin, is involved in the early stage of cell-substrate interaction', *The Journal of cell biology* 153(6): 1251-64.

Yang, J. T., Rando, T. A., Mohler, W. A., Rayburn, H., Blau, H. M. and Hynes, R. O. (1996) 'Genetic analysis of alpha 4 integrin functions in the development of mouse skeletal muscle', *The Journal of cell biology* 135(3): 829-35.

Zammit, P. S., Golding, J. P., Nagata, Y., Hudon, V., Partridge, T. A. and Beauchamp, J. R. (2004) 'Muscle satellite cells adopt divergent fates: a mechanism for self-renewal?', *The Journal of cell biology* 166(3): 347-57.

Zhang, M. and McLennan, I. S. (1995) 'During secondary myotube formation, primary myotubes preferentially absorb new nuclei at their ends', *Developmental dynamics : an official publication of the American Association of Anatomists* 204(2): 168-77.

Zhang, Y., Chen, K., Guo, L. and Wu, C. (2002) 'Characterization of PINCH-2, a new focal adhesion protein that regulates the PINCH-1-ILK interaction, cell spreading, and migration', *The Journal of biological chemistry* 277(41): 38328-38.

Ziober, B. L., Vu, M. P., Waleh, N., Crawford, J., Lin, C. S. and Kramer, R. H. (1993) 'Alternative extracellular and cytoplasmic domains of the integrin alpha 7 subunit are differentially expressed during development', *The Journal of biological chemistry* 268(35): 26773-83.

7 Eidesstattliche Erklärung

Hiermit versichere ich, die vorliegende Dissertation selbstständig und ohne unerlaubte Hilfe angefertigt zu haben.

Bei der Verfassung der Dissertation wurden keine anderen als die im Text angegebenen Quellen und Hilfsmittel verwendet.

Ein Promotionsverfahren wurde zu keinem früheren Zeitpunkt an einer anderen Hochschule oder bei einem anderen Fachbereich beantragt.

Berlin, den 25.06.2014
Maciej Czajkowski